GENETICS

Genetic determinants of blood pressure and heart rate identified through ENU-induced mutagenesis with automated meiotic mapping

Samantha K. Teixeira[1], Roberto Pontes[1], Luiz Fernando G. Zuleta[1], Jianhui Wang[2], Darui Xu[2], Sara Hildebrand[2], Jamie Russell[2], Xiaoming Zhan[2], Mihwa Choi[2], Miao Tang[2], Xiaohong Li[2], Sara Ludwig[2], Bruce Beutler[2], Jose E. Krieger[1]*

We used *N*-ethyl-*N*-nitrosurea–induced germline mutagenesis combined with automated meiotic mapping to identify specific systolic blood pressure (SBP) and heart rate (HR) determinant loci. We analyzed 43,627 third-generation (G3) mice from 841 pedigrees to assess the effects of 45,378 variant alleles within 15,760 genes, in both heterozygous and homozygous states. We comprehensively tested 23% of all protein-encoding autosomal genes and found 87 SBP and 144 HR (with 7 affecting both) candidates exhibiting detectable hypomorphic characteristics. Unexpectedly, only 18 of the 87 SBP genes were previously known, while 26 of the 144 genes linked to HR were previously identified. Furthermore, we confirmed the influence of two genes on SBP regulation and three genes on HR control through reverse genetics. This underscores the importance of our research in uncovering genes associated with these critical cardiovascular risk factors and illustrate the effectiveness of germline mutagenesis for defining key determinants of polygenic phenotypes that must be studied in an intact organism.

INTRODUCTION

Resting blood pressure (BP) and heart rate (HR) are independent factors that contribute to the risk of cardiovascular disease and mortality. The extremes of the BP distribution, low and high levels, have been linked to cardiovascular dysfunction (*1*–*4*). Similarly, HR acts as an independent predictor of mortality (*5*), and elevated HR has been associated with both cardiovascular-related and all-cause mortalities (*6*), including sudden death (*7*).

Despite the high heritability rates of BP (25 to 68%) (*8*, *9*) and HR (21 to 39%) (*10*–*12*), the identification of causal variants or associated genes through genome-wide association studies (GWAS) in human populations has been limited, revealing only a modest number of small effect variants (*13*). A GWAS meta-analysis conducted on 1 million individuals identified 901 loci associated with BP traits that explains a 10.4 mmHg increase in systolic BP (SBP) in a European population sample (*14*). This increase represents only 27% of the expected genetic contribution. Similarly, 64 loci explain only 2.5% of the total variance in HR, equivalent to a 5-bpm (beats per minute) increment (*15*).

The forward genetic screening approach addresses some of these limitations by systematically identifying numerous disease-related genes in mice (*16*, *17*). This approach capitalizes on model systems that are amenable to mutagenesis and benefits from the short generation times of mice (*18*, *19*) and zebrafish (*20*), enabling efficient high-throughput phenotypic characterization combined with mutation identification through next-generation sequencing (*17*, *21*).

In our study, we performed phenotypic screening on thousands of *N*-ethyl-*N*-nitrosurea (ENU)–mutagenized third-generation (G3) mice using automated meiotic mapping (AMM) (*17*) and machine learning assessments (*22*) to rapidly identify induced mutations affecting SBP and HR through dominant, additive, or recessive effects. Here, we present mutations in 231 candidate genes that influence SBP and/or HR, including mutations in genes previously known to affect these phenotypes, validating the efficacy of our screening. In addition, we used reverse genetics to generate knockout (KO) mice to further validate causation by a subset of mutation candidates. The comprehensive physiological and molecular characterization of model systems created for a subset of these identified genes can provide valuable insights into gene pathways and subsystems critical for the regulation of BP and HR.

RESULTS

Mapping cardiovascular quantitative traits: SBP and HR

We used AMM (*17*) combined with a dedicated software Candidate Explorer (CE) (*22*) to identify genes affecting SBP and HR (described in detail in Materials and Methods). In short, G1 males harboring 30 or more ENU-induced single-nucleotide substitutions in coding regions or splicing sites were considered as founders and were bred with C57BL/6J females, resulting in G2 mice carrying the mutations. The G2 females backcrossed with the G1 males gave rise to 30 to 100 G3 offspring per pedigree, carrying all the identified mutations in either homozygous or heterozygous states. We assessed SBP and HR using a noninvasive method of plethysmography amenable to high-throughput phenotypic screening. All animals underwent a training session on day 1, followed by two subsequent days of data collection. Each session consisted of 10 plethysmography measurements with a minimal tolerance of three good records (Fig. 1A). In total, we screened 43,627 G3 mice derived from 841 pedigrees and analyzed 45,378 variant alleles within 15,760 genes (fig. S1). Among these, 230 genes (235 alleles) and 402 genes (419 alleles) were found to be associated with SBP and HR, respectively.

We specifically focused on mutations that consistently influenced SBP or HR values in the same direction on days 2 and 3. This approach

[1]Laboratório de Genética e Cardiologia Molecular, Instituto do Coração, Hospital das Clínicas HCFMUSP, Faculdade de Medicina, Universidade de São Paulo, São Paulo, Brazil. [2]Center for the Genetics of Host Defense, University of Texas Southwestern Medical Center, Dallas, TX, USA.
*Corresponding author. Email: j.krieger@hc.fm.usp.br

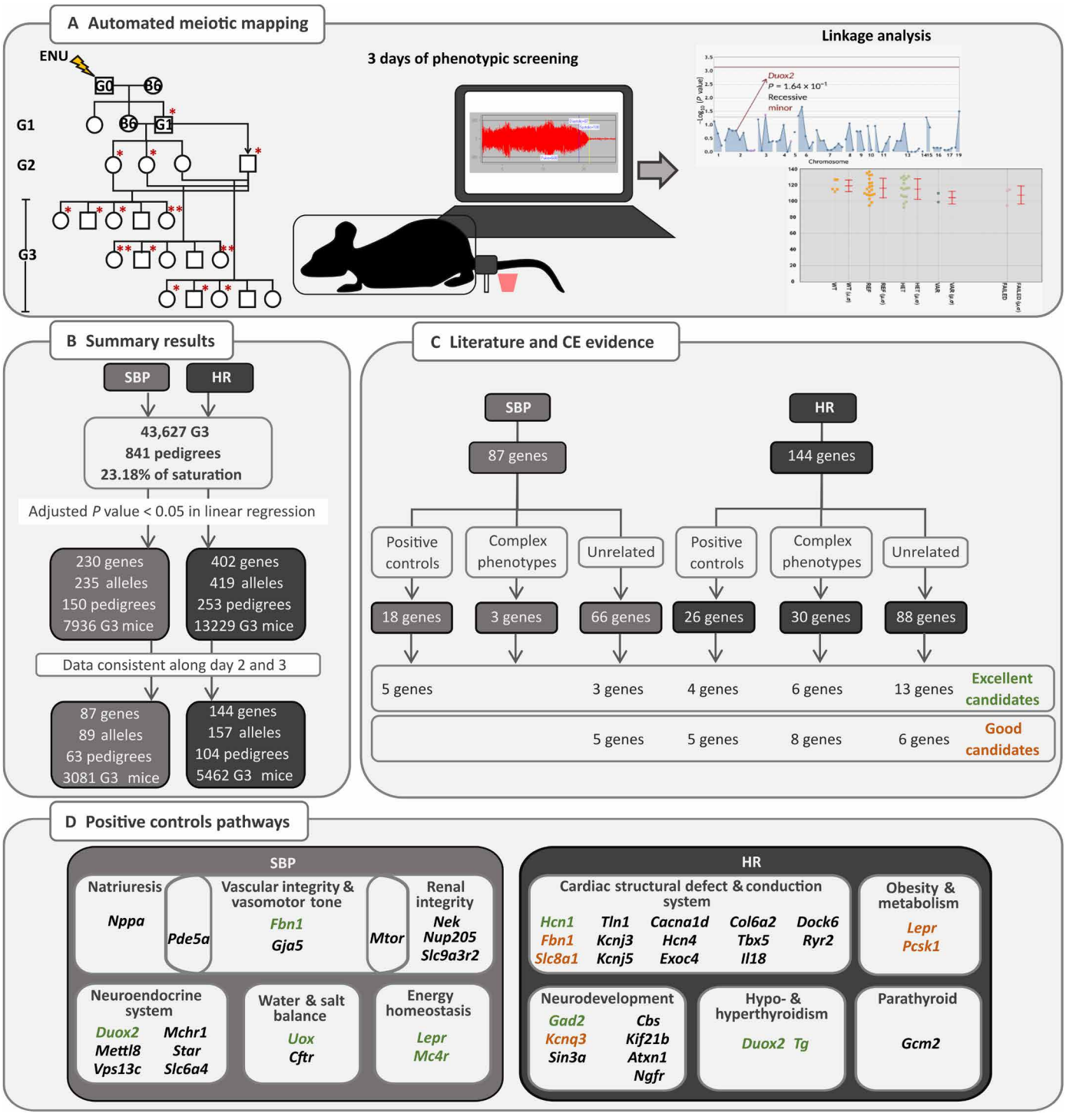

Fig. 1. Comprehensive overview of genetic screening with automated meiotic mapping. (**A**) Founder animals (G1) were characterized by whole-exome sequencing to identify ENU-induced coding variants and used to develop a pedigree of 30 to 100 mice. The zygosity of these mutations was then confirmed in the second and third generations (G2/G3) of mice before their phenotypic traits were evaluated. For measuring SBP and HR in conscious G3 mice, we used a noninvasive tail cuff method. Linkage Analyzer software used within individual pedigrees revealed significant linkage between specific mutations and changes in phenotypic scores. (**B**) Total number of G3 mice and their corresponding pedigrees assessed in our study are depicted, along with the extent of genome coverage achieved. The number of genes and alleles linked to variations in phenotypes, after refining our data analysis to include only information consistent between two consecutive days, is also shown. (**C**) Total number of candidate BP and HR genes including known genes, the ones affecting multiple systems and genes previously unrelated to BP or HR, and categorizing the gene variants as either excellent or good candidates based on a machine learning algorithm's classification. (**D**) Gene pathways influenced by the genes known to influence BP or HR. Genes marked in green were identified as excellent candidates, while those in orange were deemed good candidates by the machine learning algorithm.

led us to select 87 SBP candidates (89 alleles) out of the initially implicated 230 genes and 144 HR candidates (157 alleles) out of the initially implicated 402 genes affecting the phenotypes (Fig. 1B and tables S1 and S2). Manhattan plots [depicting statistical association(s)] revealed cosegregation of multiple mutations within peaks on several occasions, as depicted in Fig. 2A. This made it challenging to promptly identify the most likely candidate gene, although CE strongly favored one mutation over alternative mutation(s) in most of the cases. Cosegregation was observed in 44 of 87 loci associated with SBP and 84 of 144 loci associated with HR.

Regarding the 89 SBP mutations, 71 (80%) were missense mutations. According to Polyphen-2 predictions, 33 (37%) were categorized as probably damaging, 16 (18%) as possibly damaging, and 22 (25%) as probably benign. The remaining 18 mutations (20%) were classified as putative null mutations (nonsense, makesense, start loss, indels, and splicing mutations). Similarly, of the 157 HR mutations, 129 (82%) were missense mutations. Polyphen-2 predicted that 79 (50%) were probably damaging, 21 (13%) were possibly damaging, and 29 (19%) were probably benign. The remaining 28 mutations (18%) were considered putative null mutations (nonsense, makesense, start loss, indels, and splicing mutations) (fig. S1). Furthermore, most of the mutations exhibited a recessive pattern of inheritance, accounting for 60% (53 of 89 mutations) and 71.3% (112 of 157 mutations) of the cases for SBP and HR, respectively. Additive inheritance was observed in 24% (21 of 89 mutations) of SBP cases and 20.4% (32 of 157 mutations) of HR cases, while dominant inheritance occurred in 16% (15 of 89 mutations) of SBP cases and 8.3% (13 of 157 mutations) of HR cases. Last, 2 SBP and 11 HR candidate genes displayed more than one mutation associated with BP/HR changes (tables S1 and S2, respectively). In 50% of the cases, the mutations resulted in discordant phenotypes (*Neb*, an SBP gene, and *Gcm2*, *Hcn1*, *Usp34*, *Gad2*, and *Ryr2*, HR genes).

Of the 87 candidate genes associated with SBP, 8 were considered excellent candidates and 5 were deemed good candidates by CE. Similarly, among the 144 candidate mutations associated with HR, 23 were recognized as excellent candidates and 19 were classified as good candidates (Fig. 1C).

We estimated that approximately 22% of all mouse genes or specifically 23% of all autosomal genes underwent true protein-damaging mutations in at least two homozygous mice. Our assessment involved analyzing more than 45,000 mice from 800 pedigrees to determine their phenotypic characteristics (Fig. 1B). To arrive at these figures, we used a comprehensive genome saturation analysis that incorporated the Polyphen-2 algorithm and other algorithms for damage estimation, calibrated on a curated set of essential genes in which individual ENU-induced mutations unlinked to any other ENU-induced mutations were tested for lethal effects (*23*). On the basis of these calculations, we speculate that there are approximately 400 genes capable of harboring hypomorphic mutations that could affect SBP. Similarly, there may be around 600 genes in which hypomorphic mutations could potentially influence HR.

Literature-verified genes

Among the extensive list of candidate genes, only a small fraction has been thoroughly studied and established in the field. Of 87 potential genes associated with SBP, a mere 18 have been verified (Fig. 1C) and well characterized (Fig. 1D). Similarly, out of 144 candidates linked to HR, only 26 genes have been identified and adequately studied (Fig. 1, C and D).

Known genes affecting only BP

Focusing on genes specifically affecting BP, we observed that mutations in known genes contributed to increase in SBP in 50% of cases. The magnitude of these effects was comparable to that of mutations causing SBP reduction (table S3A). Unexpectedly, only five genes (*Uox*, *Duox2*, *Fbn1*, *Mc4r*, *and Lepr*) were considered excellent candidates based on CE, but among them, only *Uox* mutations were associated with increased SBP (fig. S2A and table S3A).

Examining the excellent SBP genes in more detail, two of them displayed nonsense mutations: *Uox* (*R187** in a 303–amino acid–long protein) and *Mc4r* (*Y287** in a protein consisting of 332 amino acids). Mutations in these genes were associated with the expected alterations in BP as reported in the literature, with *Uox* mutations leading to increased BP (*24*) and *Mc4r* mutations resulting in decreased BP (table S3A and fig. S2, A and B, respectively) (*25*, *26*).

Known genes affecting only HR

Among the genes affecting HR, we found that mutations in known genes caused a decrease in HR in 70% of cases. Furthermore, the magnitude of HR reduction phenotypes exceeded the magnitude of HR elevation phenotypes (table S3B). CE identified four genes (*Hcn1*, *Gad2*, *Duox2*, and *Tg*) as excellent candidates, along with five genes (*Pcsk1*, *Lepr*, *Fbn1*, *Kcnq3*, and *Slc8a1*) as good candidates (table S3B). Among these genes, three were affected by nonsense mutations: *Hcn1* (*K340** in a 910–amino acid–long protein), *Gad2* (critical splicing site alteration resulting in a 108-nucleotide deletion of exon 14, predicting an in-frame deletion of 36 amino acids after amino acid 462), and *Tg* (*C2452** in a protein consisting of 2766 amino acids) (table S3B and fig. S2, C to E). In addition, missense mutations in these genes were also associated with the HR phenotype; however, they resulted in opposing phenotypic changes in the cases of *Hcn1* and *Gad2* genes (table S3B and fig. S2, C and D).

Known genes affecting both phenotypes

Mutations in three excellent/good candidate genes have been identified to affect multiple phenotypes. A missense mutation (*H1110D*) in the *Duox2* gene was found to be associated with lower SBP, HR, and body weight. This mutation cosegregated precisely with a missense mutation in *Zfp106*, making it challenging to determine the direct cause and effect relationship [Figs. 2A and 3A and table S3 (A and B) for *Duox2* and Fig. 3C and table S5 (A and B) for *Zfp106*, regarding the SBP and HR phenotypes, respectively]. In another pedigree, a separate variant allele of *Duox2* with the amino acid change *Q1341R* was observed. Homozygosity for this second variant allele resulted in decreased HR and body weight but without significant changes in SBP (Figs. 2B and 3A).

In addition, a *Lepr* missense mutation causing the amino acid change *P874T* was found to cause a recessive decrease in SBP and HR, as well as weight gain (fig. S3A and table S3, A and B). *Lepr* and *Mc4r* are both part of the leptin-melanocortin pathway, which plays a critical role in energy balance. Studies using KO mice and experimental models have demonstrated that deletion of *Mc4r* or *Lepr* is associated with lower BP, obesity, and sympathetic inhibition (*27*, *28*).

Last, an *Fbn1* missense mutation (*C2320R*) was associated with lower BP and HR (Fig. 3B and table S3, A and B). Mutations in *Fbn1* are known to cause Marfan syndrome, a connective tissue disorder that predisposes individuals to musculoskeletal, ocular, and cardiovascular abnormalities, including aortic rupture, dissection, and congestive heart failure (*29*). It has been reported that patients with

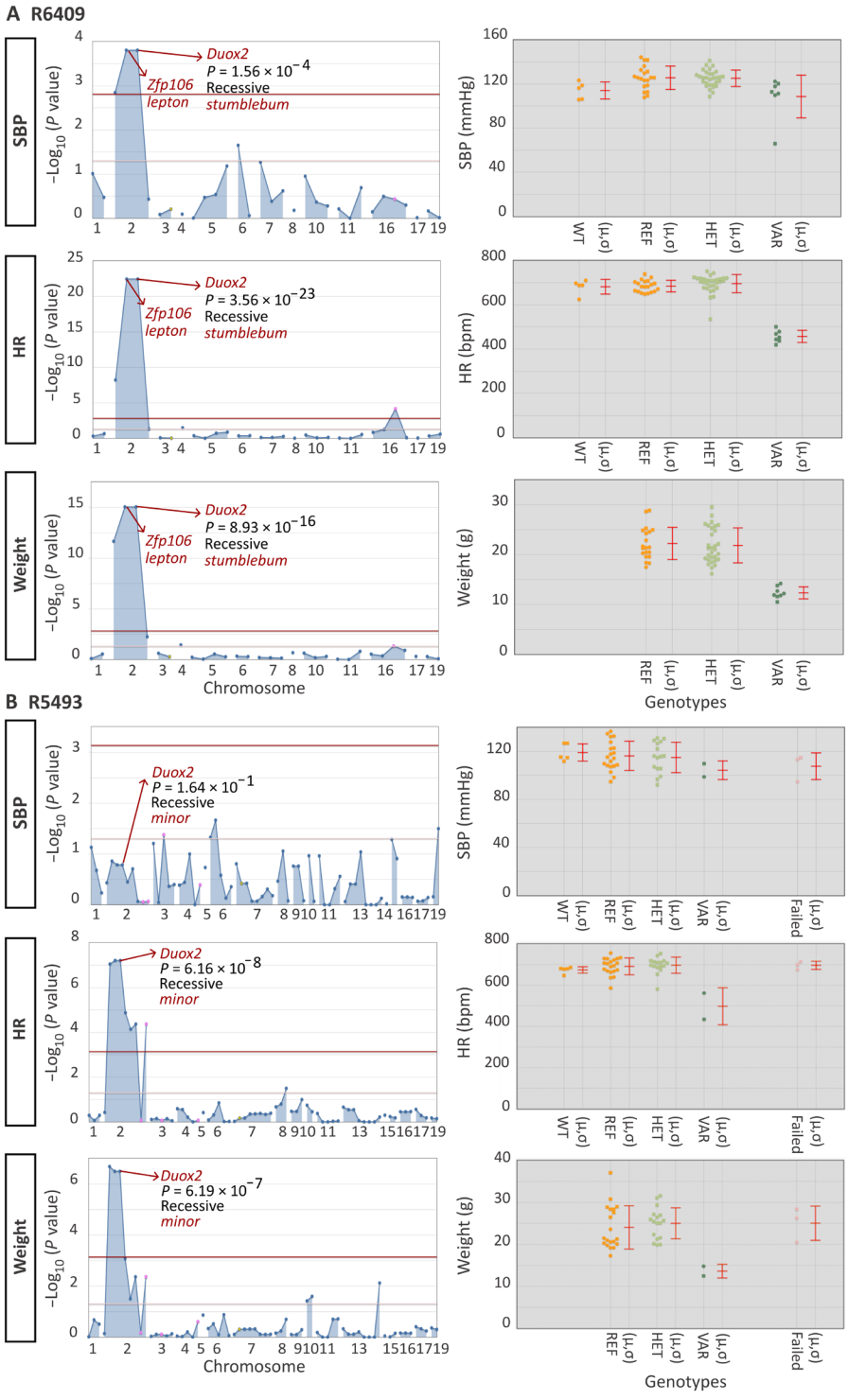

Fig. 2. *Duox2* linkage analysis that displays pleiotropic effects. Linkage analysis data for each pedigree depicted by Manhattan plots. The *y* axis displays the negative logarithm of the *P* value (−$\log_{10}$ *P* value), while the *x* axis indicates the chromosomal locations of mutations identified in the G1 founder of each pedigree. Gene names, *P* values, modes of inheritance, and allele names are shown where applicable. Red and beige lines signify the *P* value thresholds of 0.05, with and without Bonferroni's correction, respectively. The scatterplots summarize the average SBP [in millimeters of mercury (mmHg)] and HR [beats per minute (bpm)] measurements over two consecutive days, as well as weight [in grams (g)]. Genetic backgrounds are color-coded: C57 control mice (WT, orange), homozygous WT littermates (REF, orange), heterozygous littermates (HET, light green), and homozygous mutated mice (VAR, dark green). Each data point corresponds to an individual mouse, and we also display the mean (μ) and SD (σ) for these values. Instances labeled "Failed" indicate unknown genotypes resulting from unsuccessful genotyping reactions. (**A**) *Duox2* allele in R6409 pedigree: The *stumblebum* mutation affects BP, HR, and weight. (**B**) *Duox2* allele in R5493 pedigree: The *minor* mutation influences only HR and weight.

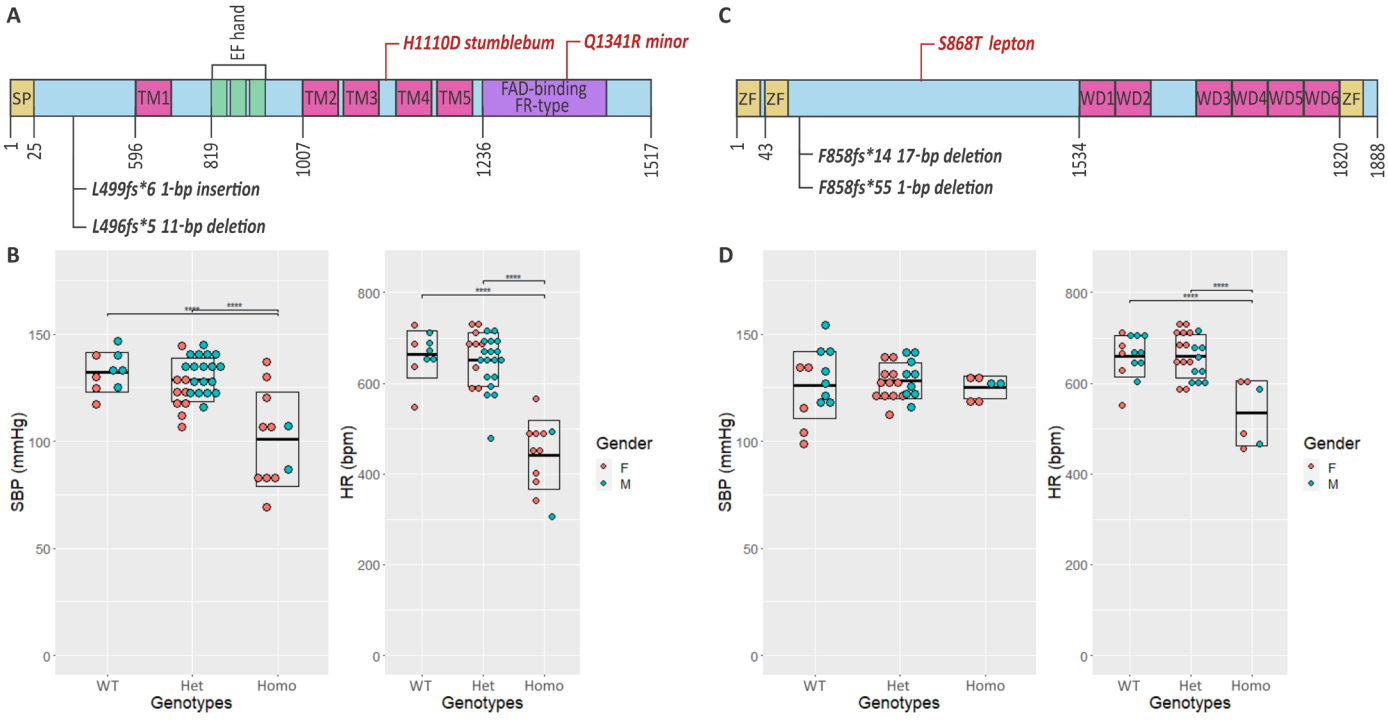

Fig. 3. Dissecting the cosegregation between Duox2 and Zfp106 alleles on SBP, HR, and weight phenotype using reverse genetics. (**A** and **C**) The image illustrates the structure of the mouse protein, highlighting the ENU (red) and KO (black) alleles. (**B** and **D**) It also shows the SBP and HR data, gathered over two consecutive days using plethysmography, to compare different genotypes in mice from KO strains developed for *Duox2* and *Zfp106* genes. Each dot signifies an individual animal, while the boxes indicate the average value ± SD. A significant *P* value of less than 1×10^{-4} is noted in the posttest analysis. The protein domains are labeled as follows: TM, transmembrane; SP, signal peptide; EF hand, calcium-binding domain; FAD-binding FR type, domain associated with ferric reductase NAD binding; ZF, N-terminal zinc finger; WD, the WD40 repeat domain. Gender: F, female; M, male.

Marfan syndrome experience hypertension (*30*, *31*), increased HR (*32*), and reduced HR recovery after exercise (*33*), suggesting autonomic dysfunction.

Genes with secondary involvement in SBP and HR phenotypes

We have identified genes associated with conditions or syndromes that can affect pathways or systems leading to changes in BP and HR. However, direct evidence linking these genes to BP and HR alterations is lacking. Among the genes, we identified three SBP genes with mutations found in patients with diseases causing substantial cardiac defects, such as Carpenter [*Megf8* (*34*)] and Noonan syndrome [*Lztr1* (*35*)] (fig. S4A and table S4A). However, there is no evidence of BP alterations in these diseases. In addition, none of these genes were considered excellent or good candidates according to CE (Fig. 1C).

In contrast, we found 30 HR genes with mutations or common variants associated with diseases where HR alteration may be a secondary effect. Most of these genes (21 of 30) are involved in neurodevelopmental diseases that have an extensive phenotype but no evidence of HR alteration (Fig. 1C and fig. S4A). Fifty percent of these genes (10 of 21) were considered excellent or good candidates by CE (fig. S4A and table S4B).

One of these excellent candidates, *Ap4e1*, showed a recessive increase in HR due to a null mutation causing a start codon loss in our study (table S4B). Mutations in this gene lead to autosomal recessive spastic paraplegia 51 (SPG51), a neurodegenerative disorder characterized by intellectual disability, speech and movement disorders, and, in some cases, seizures (table S4B) (*36*). However, a recent study by Spielmann *et al.* (*37*) using transthoracic echocardiography (TTE) on *Ap4e1* KO mice demonstrated that homozygous loss-of-function mutations in *Ap4e1* actually cause a decrease in HR and an increase in the time between two successive R waves on the ECG (RR interval), showing an opposite phenotype to what we reported. The underlying mechanism by which this gene causes HR alteration remains unknown.

The remaining genes we identified were associated with cardiac structural and/or conduction system defects (three genes), heart disease (four genes), or hypo- and hyperthyroidism (two genes). Four of these nine genes were considered excellent or good candidates (Fig. 1C and fig. S4A). Nevertheless, the relationship between these genes and phenotypes is not clearly understood. For instance, we observed missense mutations in *Usp34* associated with both HR increase and decrease (table S4B). Szot *et al.* (*38*) also identified a likely pathogenic variant in the *USP34* gene that segregates with congenital heart disease in a study involving three families and whole-exome sequencing, but the influence of this gene on the disease is unclear.

We also discovered a significant association between the $Nae1^{D208G}$ allele and a recessive increase in HR (pedigree R6318; fig. S4B and table S4B). This allele was not considered a good candidate by CE. Muffels *et al.* (*39*) reported a biallelic variant in *NAE1* associated with a neurodevelopmental disorder characterized by dysmorphic faces and ischiopubic hypoplasia.

To validate the association of *Nae1* with the HR phenotype, we engineered two strains of mice. The first strain contained a missense mutation (*C294G*) resulting from a 1–base pair replacement, while the second strain had a frameshift mutation caused by a 4–base pair deletion. The frameshift mutation led to a protein alteration starting at amino acid 297, with the inclusion of eight abnormal amino acids followed by a stop codon (*I297fs*8*) (fig. S4C). Because the $Nae1^{I297fs*8}$ mutations were lethal, we did not develop homozygous mice for this allele. As a result, all engineered homozygous mice were either homozygous for the missense allele *C294G* or compound heterozygotes for both alleles (fig. S4D). In contrast to the observations from the forward genetic screening, altering the Nae1 protein resulted in a recessive decrease in HR (fig. S4D and table S6A).

Neddylation is a process similar to ubiquitination, where the ubiquitin-like protein NEDD8 is conjugated to specific protein targets using E1-E2-E3 enzymes. It has recently emerged as a previously unknown regulatory mechanism controlling various cellular functions, including transcriptional regulation, cell cycle progression, and differentiation. E1 consists of a heterodimer of NAE1 and UBA3 proteins, which activate NEDD8 in an adenosine 5′-triphosphate (ATP)–dependent manner (*40*). NEDD8 is highly expressed in the heart, particularly in skeletal and cardiac muscles, compared to other organs (*41*, *42*). Furthermore, neddylation enzymes and neddylated proteins are highly expressed in embryonic hearts but significantly down-regulated 1 week after birth (*41*). Mice lacking *Nae1* exhibit reduced neddylation, myocardial hypoplasia, and ventricular noncompaction due to dysregulation of cell cycle–regulatory genes and inhibition of cardiomyocyte proliferation both in vivo and in vitro. These effects can lead to heart failure and perinatal lethality. Consistent with our engineered mouse model, *Nae1* KO mice also display decreased HR compared to control mice. Previous studies have demonstrated that neddylation is essential for proper cardiac development by inhibiting the Hippo pathway and activating yes-associated protein signaling, which are crucial for cardiac morphogenesis (*41*).

Recently, it was shown that the administration of a specific and potent inhibitor of NAE, MLN4924, on postnatal days 1, 3, and 5 resulted in modest neddylation inhibition. This led to a reduction in cardiomyocyte proliferation, the development of cardiac dysfunction and hypertrophy, and a significant decrease in HR on postnatal day 7. Therefore, the neonatal cardiomyopathy resulting from MLN4924 suggests that even modest and transient inhibition of neddylation during key phases of heart development can be detrimental to cardiac structure and function (*43*).

In summary, it appears that the lack of *Nae1* gene product, as previously described and also observed in our CRISPR model, is associated with decreases in HR, while the more discrete ENU-induced variant is associated with HR increases. These findings provide additional evidence supporting the involvement of *Nae1* in heart development and the HR phenotype. However, the complex neddylation influence is timing and context dependent, resulting in a wide range of HR phenotypes.

Validation of candidate BP and/or HR genes using reverse genetics

Dissecting the cosegregation between Duox2 and Zfp106 alleles on BP, HR, and weight phenotype

We identified a significant association between the $Duox2^{H1110D}$ allele, also known as *stumblebum*, in a recessive mode and a decrease in SBP, HR, and body weight (Fig. 2A; pedigree R6409). The $Duox2^{H1110D}$ allele cosegregated with a *Zfp106* allele ($Zfp106^{S868T}$), named *lepton*, which made it challenging to promptly identify the responsible gene for these phenotypes [Figs. 2A and 3 (A and C) and table S5 (A and B)]. In addition, we found a significant association between the $Duox2^{Q1341R}$ allele, named *minor*, and a recessive decrease in HR and weight only (Figs. 2B and 3A).

The *Duox2* gene serves as a positive control for BP and HR due to the established evidence that inactivating mutations in the *DUOX2* gene in humans are associated with permanent and transient congenital hypothyroidism (*44*). Thyroid hormones have wide-ranging homeostatic effects, particularly targeting the cardiovascular and neuroendocrine systems. For example, hypothyroidism is accompanied by increased systemic vascular resistance, vascular permeability, and catecholamine levels, as well as decreased blood volume, arterial compliance, density of β-adrenergic receptors, plasma renin activity levels, aldosterone levels, cardiac output, and HR (*45*). Hence, the phenotype observed in pedigree R6409 aligns with an altered *Duox2* allele (table S3, A and B). *Duox2* KO mice confirmed the results of the ENU mutation screening, exhibiting decreased SBP, HR, and body weight (Fig. 3, A and B, and table S6B), consistent with the previously reported dwarfism (*46*).

$Zfp106^{S868T}$ is a strong candidate for influencing HR regulation by CE score (table S5B). To validate the association with *Zfp106*, we used engineered *Zfp106* KO mice (Fig. 3C), which resulted in a recessive decrease in HR and body weight, while SBP remained unchanged (Fig. 3D and table S6C). These findings indicate that the $Zfp106^{S868T}$ allele affects HR and body weight phenotypes, while SBP is specifically affected by the $Duox2^{H1110D}$ allele, as observed in the data from pedigree R6409. Furthermore, this demonstrates the power of CE in selecting strong candidates for further investigation.

The *Zfp106* gene encodes a zinc finger protein highly expressed in muscle (skeletal muscle and heart) and brain. It has recently been found to localize to nuclear speckles and interact with the core splicing factor RBM39, playing a role in the postnatal maintenance of myofiber innervation by motor neurons. Previous observations using *Zfp106* KO mice demonstrated muscle wasting and a significant reduction in hindlimb skeletal muscle weight compared to wild-type (WT) littermates, without a significant decrease in body weight (*47*). On the basis of these findings, we speculate that knocking out the *Zfp106* gene also affects the myofiber innervation of cardiac muscle, which is consistent with the observed decrease in HR.

Mouse model of aging causing alteration in BP and HR

We also discovered a significant recessive association between the Kl^{M689K} allele (referred to as *anatolia*) and a decrease in HR (Fig. 4, A and B, and table S5B). To confirm the link between *Kl* and the HR phenotype, we engineered two strains: The first strain had a single–base pair replacement resulting in a missense mutation causing the alteration of the same amino acid by ENU (*M689L*), while the second strain had a 1–base pair insertion leading to a frameshifted protein starting from amino acid 689. This frameshifted protein included 28 aberrant amino acids and terminated with a stop codon (*M689fs*28*) (Fig. 4B).

Besides validating the initially identified HR phenotype, these engineered strains also exhibited altered SBP and body weight (Fig. 4C and table S6D). These findings are consistent with what has been reported in other KO models of *Klotho*, as described below.

Initially characterized as an anti-aging factor, Klotho is known to play a crucial role in various physiological processes. Lack of *Klotho* expression results in a syndrome resembling human aging,

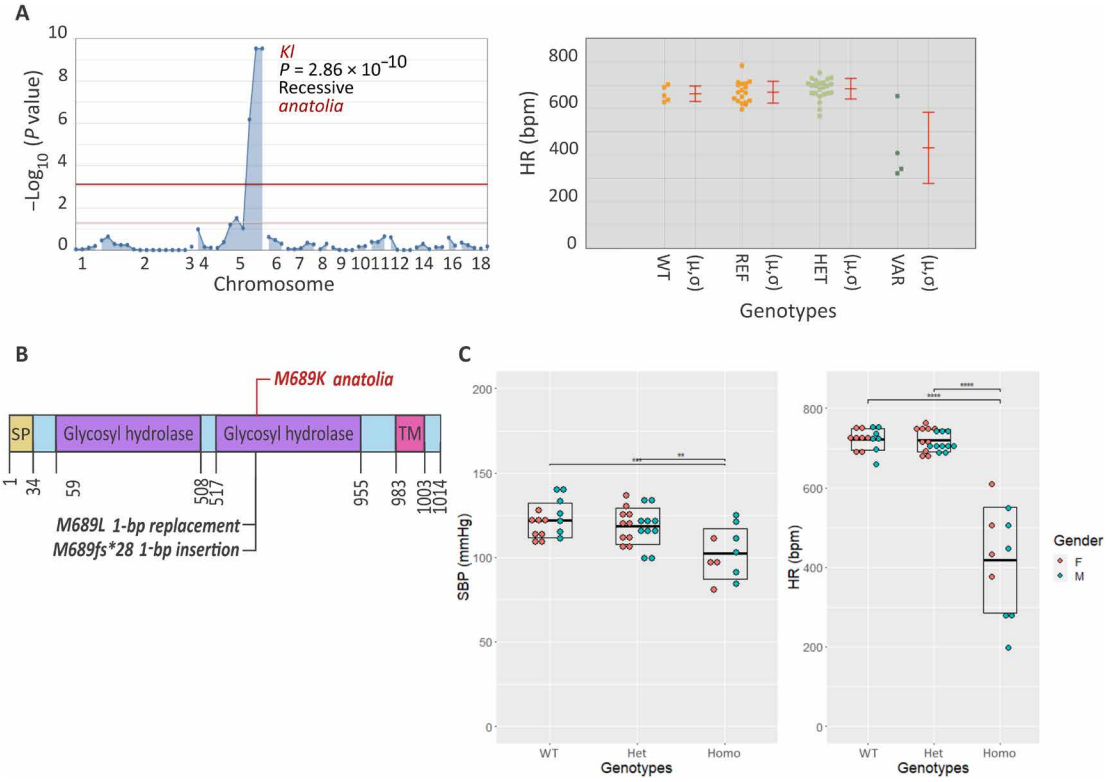

Fig. 4. *Kl* linkage analysis and validation using reverse genetics. (**A**) Manhattan plot for linkage analysis data and scatterplot showing the average HR over two consecutive days in mice identified during the ENU screen in pedigree R6158. The Manhattan plot shows $-\log_{10} P$ values (calculated using a recessive transmission model) on the *y* axis against the chromosomal positions of mutations identified in the G1 founder on the *x* axis, with linkage peaks annotated with gene name, *P* value, inheritance mode, and allele name. Red and beige lines indicate *P* value thresholds of 0.05, with and without Bonferroni's correction, respectively. The HR data (in bpm) is plotted against genotype for the *Kl*-specific mutation. The scatterplot, from left to right, shows C57 control mice (WT, orange), homozygous WT littermates (REF, orange), heterozygous littermates (HET, light green), and homozygous mutants (VAR, dark green), with each point representing one mouse. The mean (μ) and SD (σ) are also shown. (**B**) Protein domain diagram for Kl, highlighting the ENU-mutated residue and allele name in red and engineered alleles in black. The protein domains are labeled as follows: (**C**) SBP and HR data collected over two consecutive days using plethysmography across different genotypes of mice from engineered strains for the *Kl* gene. Each data point represents one animal, with boxplots showing the mean ± SD. Statistical significance is indicated with asterisks: $^{**}P < 1 \times 10^{-2}$, $^{***}P < 1 \times 10^{-3}$, and $^{****}P < 1 \times 10^{-4}$ in posttest analysis.

characterized by normal development for the first 3 weeks, followed by growth retardation, atrophy of genital organs and thymus, arteriosclerosis, ectopic calcification, osteoporosis, and premature death (*48*). The gene is highly expressed in the kidney, parathyroid gland, and choroid plexus, and it encodes different isoforms: a transmembrane protein, a soluble protein produced through cleavage, and a truncated soluble protein produced through alternative splicing (*49*). The transmembrane protein acts as a receptor for Fgf23, inducing phosphaturia, down-regulation of the vitamin D–regulatory hormone, and compromising salt-handling by the kidney (*50*, *51*).

Both *Fgf23*-deficient mice and *Klotho*-deficient mice exhibit similar phenotypes, including renal sodium wasting, hypovolemia, and decreased BP. Conversely, haplodeficiency of the *Kl* gene has been shown to induce renal damage and hypertension, possibly through the up-regulation of the *Cyp11b2* gene, which increases aldosterone synthesis (*52*). Furthermore, down-regulation of *Kl* in the intracerebroventricular region of Wistar Kyoto rats impairs baroreflex BP regulation (*53*). In addition, Klotho may directly influence HR by affecting sinoatrial node function (*54*).

Mouse model of vascular integrity causing alteration in BP

We observed a decrease in SBP in homozygous mice with a mutation in the *Notch3* gene compared to heterozygous and WT littermates (Fig. 5, A and B, and table S5A). This mutation, called *divide*, may cause aberrant splicing, resulting in a transcript with a 71-nucleotide deletion in exon 28. This deletion leads to a frameshift in the 2318–amino acid–long protein at amino acid 1706, ultimately terminating after the inclusion of 5 abnormal amino acids (Fig. 5B). To validate the association between *Notch3* and BP phenotype, we developed two KO strains. One strain contains a 16–base pair deletion, resulting in a frameshifted protein starting from amino acid 58, with the inclusion of 96 abnormal amino acids followed by a stop codon (*Q58fs*96*). The second strain contains a 2–base pair insertion, leading to a frameshifted protein starting from amino acid 61, with the inclusion of 99 abnormal amino acids followed by a stop codon (*S61fs*99*) (Fig. 5B). Despite the fact that CRISPR targeting abrogates the entire Notch3 protein compared with the discrete changes associated with ENU-induced mutagenesis, both resulted in a decrease in SBP when in recessive mode (Fig. 5C and table S6E), suggesting that deletion of the intracellular domain suffices to decrease BP levels.

Notch3 is a member of the Notch family and functions as a receptor for membrane-bound ligands Jagged1 and Jagged2, as well as delta-like 1, 3, and 4. Upon ligand binding and activation, Notch undergoes two proteolytic cleavages, releasing the extracellular and intracellular domains (ECD and NICD, respectively). The NICD is

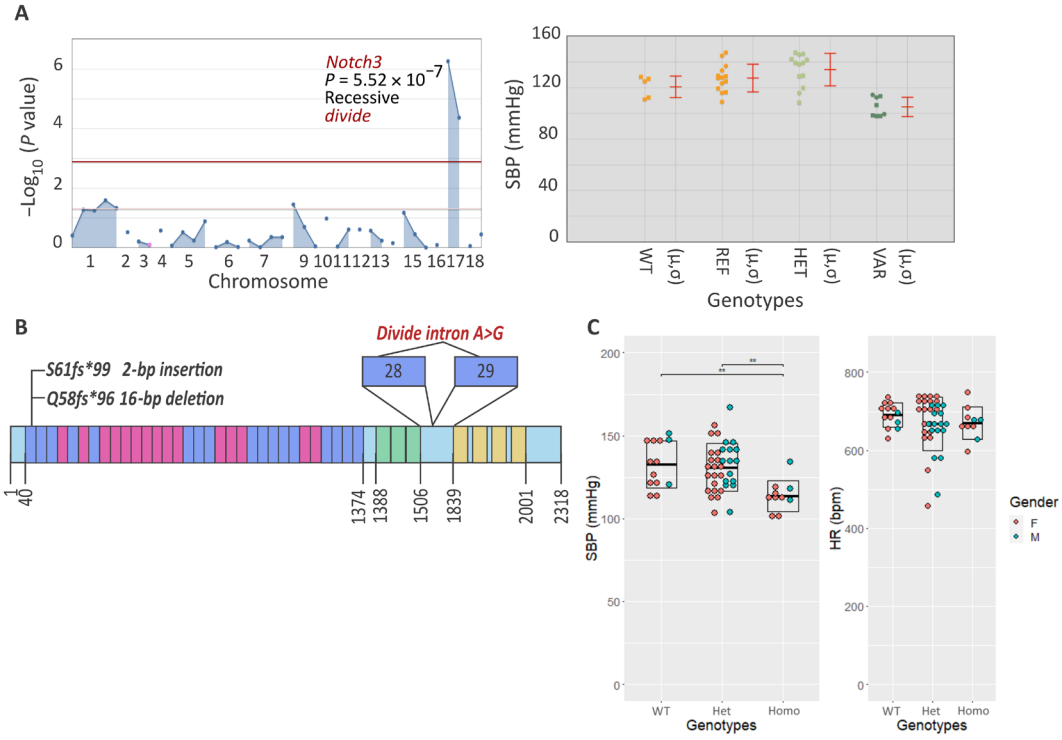

Fig. 5. *Notch3* linkage analysis and validation using reverse genetics. (**A**) Manhattan plot illustrating linkage analysis data, alongside a scatterplot showing the average SBP measurements (in mmHg) taken over two consecutive days in mice identified by the ENU screen in pedigree R6316. This mutation was found to be significantly associated with SBP as indicated. (**B**) The diagram illustrates the protein domain structure of Notch3, highlighting both the ENU-mutated residue (shown in red) and engineered alleles (depicted in black). The ENU mutation may cause aberrant splicing, resulting in a transcript with a 71-nucleotide deletion in exon 28. The protein domains are color-coded as follows: blue for EGF like, pink for EGF-like calcium binding, light green for the notch domain, and yellow for ankyrin repeats. (**C**) SBP and HR data, averaged over two consecutive days, obtained through plethysmography in different genotypes of mice from both *Notch3* KO strains. Each data point represents an individual animal, while the boxes indicate the mean ± SD. A *P* value of less than 0.01 (1×10^{-2}) was noted in the posttest analysis. Gender: F, female; M, male.

involved in differentiation, proliferation, and apoptotic events at all developmental stages (*55*). Extensive evidence suggests that Notch3 primarily affects the vascular smooth muscle and its function and structure. Notch3 influences the identity, proliferation, and apoptosis of vascular smooth muscle cells (vSMCs) (*56*–*58*), and its expression appears to be restricted to vSMCs in adult human tissues (*59*). *Notch3*-deficient mice exhibit structural defects in distal arteries and altered myogenic response, and these phenotypes are a result of the deficient arterial specification of vSMCs (*58*). In addition, Boulos *et al.* (*60*) demonstrated that the absence of *Notch3* compromises renal vascular reactivity in mice, resulting in an inadequate adaptation of renal resistance vessels to abrupt changes in SBP or the cardiac and renal damage associated with chronic exposure to angiotensin II, despite reduced BP levels. In humans, mutations in the *NOTCH3* gene cause CADASIL, a cerebral autosomal dominant arteriopathy that leads to dementia and stroke associated with white matter abnormalities (*61*). Conversely, it has been observed that the overexpression of *Notch3* in the lungs of mice with pulmonary hypertension can be reversed by treatment with a γ-secretase inhibitor, which blocks Notch3 signaling in vSMCs. Furthermore, the absence of the *Notch3* gene prevents pulmonary hypertension induced by hypoxia (*62*).

In previous studies, the BP differences between KO and WT mice were not observed in basal conditions. This may be related to the complete abrogation of the *Notch3* gene product reported here compared to the more discrete changes in the gene product reported previously, affecting only part of the extracellular domain. Of note, the latter mutation recapitulates better the CANDASIL phenotype observed in human (*63*). We speculate that the lower SBP levels are consistent with disrupted vSMC development, lower peripheral resistance, and reduced susceptibility to target organ damage.

IMPC data providing additional validation for the SBP and HR candidates

In their recent study, Spielmann *et al.* (*37*) examined 3894 single-gene–null mouse strains from the International Mouse Phenotyping Consortium (IMPC) using electrocardiography (ECG) and TTE. They wanted to identify genes responsible for structural and functional cardiac abnormalities. We cross-verified our findings and identified that 13 of 87 SBP candidates and 30 of 144 HR candidates were also examined in the IMPC database.

Focusing on HR, four genes with null mutations exhibited HR phenotype changes: *Kcnj3*, *Ap4e1*, *Gpr153*, and *Fbxo24* (table S7A). Notably, *Kcnj3* served as a positive control, with both ENU and IMPC null mice showing increased HR compared to their WT counterparts. *Ap4e1* and *Gpr153*, indirectly involved in HR regulation, presented contrasting phenotypes: ENU mice exhibited HR increases, while IMPC null mice showed increased interval between the end of the S wave and the beginning of the T wave on the ECG (ST interval) and

decreased HR in *Gpr153* and *Ap4e1*, respectively. *Fbxo24*, a previously unknown HR regulation candidate, demonstrated consistent HR increases in both studies (table S7A).

Although Spielmann *et al.* (*37*) did not directly assess BP, changes in heart structure and function may result from pressure overload. In this context, *Vps13c*, a positive control, showed increased left ventricular posterior wall thickness in the IMPC study, aligning with our findings of elevated BP (table S7B). In addition, the IMPC's ECG and TTE results for the identified genes *Rsbn1* and *Nrxn1* imply their influence on BP. For instance, increased ejection fraction and reduced end-systolic diameter in *Nrxn1* mutants could result from decreased afterload due to lower BP, while a significant BP increase in *Rbsn1* mutants might heighten parasympathetic activity, counteracting BP changes observed in both ENU and IMPC null mutants (table S7B).

In summary, Spielmann *et al.*'s work (*37*) corroborates the significance of seven candidate genes identified in our forward genetic screening, furthering the potential to improve our understanding of cardiovascular abnormalities at the genetic level.

GWAS catalog highlighting potential human translational targets

Our study explores further into how many candidate genes identified in the mouse model using AMM have corresponding human orthologs located near genome-wide significant associations for BP and HR traits, as indicated in the GWAS catalog. Of the 87 BP candidate genes, 79 have human orthologs and 15 are in proximity to 40 single-nucleotide polymorphisms (SNPs) significantly linked with BP traits. This is within a broader context of 9369 significant associations and 4552 SNPs near 4047 genes (table S8). In the case of the 144 HR candidate genes, 140 have human orthologs and 18 are close to 62 SNPs significantly associated with HR traits, taken from a total of 3669 significant associations and 2147 SNPs near 2006 genes (table S9).

Furthermore, we noted a significant enrichment of our candidate genes among those genes mapped near SNPs identified in GWAS for both BP and HR traits. This was evidenced by P values of 0.032 and 5.6×10^{-4} for BP and HR-related traits, respectively, in hypergeometric tests, considering only coding genes.

DISCUSSION

The genetic architecture underlying complex cardiovascular traits remains poorly understood, but results from our study provide valuable insights. Here, we present a comprehensive strategy and compelling findings elucidating genes that may be involved in pathways and subsystems influencing BP and HR phenotypes. By examining 841 pedigrees comprising 45,261 G3 mice and analyzing more than 45,000 ENU mutations, which collectively damage 22% of the mouse genome so as to cause detectable phenovariance in those genes supporting normal functions placed under surveillance, we have identified 87 candidate genes associated with SBP and 144 candidate genes associated with HR.

Among the identified candidates, 18 genes related to SBP and 26 genes related to HR have already been implicated in BP or HR regulation. However, the remaining 69 SBP candidates and 118 HR candidates have not yet been linked to these phenotypes, presenting an exciting opportunity for insights into BP and HR regulation.

Animal models have played a substantial role in replicating and analyzing the genetic makeup of complex traits. In the late 1950s, specific rat strains were created in which alleles associated with hypertensive, hypotensive, or salt-sensitive traits were fixed by selectively breeding pairs with extreme phenotypes. Decades later, using genome-wide molecular markers, we and others mapped BP quantitative trait loci that contained genes influencing BP using these rat strains (*13*, *64*). These regions were subsequently segregated through backcrossing, leading to the development of congenic and consomic strains. Although this approach initially showed promise in transferring candidate regions and expected phenotypic characteristics, it proved to be laborious and resulted in the identification of only a few genes involved with the expected trait characteristics. Further investigation revealed that the complexity of the rat genome and the interactions among different chromosomal regions hindered the prompt and definitive identification of critical BP genes. Nevertheless, these rat strains have served as valuable supporting evidence for the involvement of candidate genes, as indicated in the present study. Our study detected similar BP changes to those observed in successful congenic strains (*65*). For instance, mutations in the *Lepr* and *Mc4r* genes were associated with a decrease of 30 to 40 mmHg in BP levels in homozygous var mice compared to ref mice.

We have also identified genes that are associated with conditions or syndromes affecting pathways or systems that can ultimately lead to changes in BP and HR, although direct evidence is lacking. Our findings were particularly notable in relation to HR genes, as we discovered that 21% of HR genes (30 of 144) exhibited genetic variations associated with syndromes in the ClinVar database. Most of these syndromes are related to neurodevelopmental diseases that result in extensive phenotypic effects. Thus, in addition to the pathways regulating action potential in the heart, pacemaker function, and heart contractility, the central nervous system plays a crucial role in HR regulation and is associated with changes in heart rhythm. However, investigating the effects of these genes on HR is challenging due to their pleiotropic effects when disrupted or their essentiality, which can lead to lethal phenotypes.

We observed discordant phenotypes between different ENU mutations in half of the genes with more than one mutation, as well as between ENU and KO mutations. For instance, an ENU mutation in the *Nae1* gene led to an increased HR, while our engineered mice with a missense mutation in the same gene exhibited a decreased HR. Both mutations followed a recessive inheritance pattern. Consistent with this fact, Spielmann *et al.* (*37*) investigated a *Nae1* null allele (*Nae1<tm1b(EUCOMM)Wtsi>*) in heterozygosity due to the gene's essentiality, but no alteration in HR phenotype was observed (*37*). This phenotypic discordance between ENU-induced and engineered alleles was also observed for the HR candidate gene *Ap4e1* developed by IMPC. The concept of phenotypic heterogeneity arising from mutations in the same gene has been observed both in experimental models and in various human genetic disorders. This variability manifests as incomplete penetrance or differing levels of expressivity. These phenomena are influenced by several factors. First, the characteristics of the causal variants, such as their position in the protein and subsequent impact on protein function, play a crucial role. Second, the mutation's effect on gene expression is substantial. This includes variations in allelic expression, impacts on different protein isoforms, interactions with cis/trans elements, and epigenetic factors. Last, global modifiers also contribute, encompassing genetic background and compensatory mechanisms (*66*).

Moreover, studies involving gene overexpression and downregulation through transgenic mice and small interfering RNA

(siRNA) have shown that the phenotypes observed with these manipulations do not always replicate or confirm data from KO mice (*27*). This limitation is important to acknowledge in our strategy since the development of KO mice is the primary approach for confirming findings from the forward genetic screening. Our study's use of ENU mutations, despite some limitations, presents a distinct advantage. These mutations offer a unique means to explore both loss- and gain-of-function alterations in specific genes and assess their effects on phenotypes. This approach is particularly valuable considering the more labor-intensive and less efficient process of creating knock-in mice using CRISPR, although it is achievable. In addition, examining the phenotypic diversity resulting from multiple ENU mutations in the same gene provides deeper insights into the nuances of incomplete penetrance and variable expressivity, especially relevant in the study of complex and polygenic phenotypes.

In light of efforts to understand the genetic architecture of complex cardiovascular traits, the knowledge gained from human studies is somewhat underwhelming. Despite studying millions of individuals, the identified SNPs associated with BP and HR traits explain only a modest 5.7% (*14*) and 2.5% (*15*) of the variances in SBP and resting HR, respectively. Unexpectedly, the weighted genetic risk score (GRS) for BP, considering all 901 loci identified in a large GWAS meta-analysis, is associated with just a 10.4 mmHg increase in the UK population (*14*). The GRS effect size is comparable to that of single mutation reported in one gene in our study, which primarily investigates the coding regions of genes influencing cardiovascular phenotypes. In contrast, the variants identified through GWAS are predominantly located in noncoding DNA regions enriched in regulatory elements (*67*).

Our findings suggest that genes in proximity to SNPs significantly linked to BP and HR traits in GWAS could play a causal role. This highlights the importance of investigating genetic variants that affect the expression and splicing of these candidate genes, particularly in tissues that regulate BP and HR. Such research could reveal pathways or subsystems unknown to be involved in hypertension and arrhythmia disorders. However, caution is warranted when using our data to assign human genes influencing BP and HR phenotypes, as our study covers only 22% of the mouse genome. In addition, the lack of a significant association between mutations in a gene deemed fully analyzed and the studied phenotypes does not rule out its potential as a candidate gene. This is because our saturation estimation is based on loss-of-function mutations, and rare gain-of-function alleles might still have an impact on phenotypes.

BP and HR traits, along with associated diseases such as hypertension and arrhythmia, are multifactorial and substantially influenced by genetics. The polygenic nature of these traits and their association with disease risk encompass a wide range of influences, ranging from a few to hundreds of gene variants with varying individual contributions (*68*). While GWAS have been instrumental in mapping and identifying numerous common genetic variants associated with specific traits or diseases, the individual contribution of each variant tends to be small. In contrast, the identification of rarer variants with moderate to large contributions remains largely unknown, despite their potential to explain the missing heritability (*69*). The task of identifying these rare variants is challenging, as evidence suggests that it may require sequencing between 75,000 and 185,000 cases to identify a rare variant with exome-wide significance for type 2 diabetes (*70*). In this context, the data presented here contribute to expanding the list of candidate genes with loss- or gain-of-function mutations that affect BP and HR, potentially shedding light on hypertension and arrhythmias, complementing the results of genome-wide searches that require a large number of human cases.

Together, these findings provide insights and elucidate on the underlying mechanisms and subsystems contributing to the development of critical cardiovascular risk factors. Moreover, they underscore the effectiveness of germline mutagenesis as a tool for defining key determinants of polygenic phenotypes that must be studied in an intact organism.

MATERIALS AND METHODS

All procedures were approved by the University of Texas Southwestern Medical Center (animal protocol number 2011-0145) and the University of São Paulo Medical School Institutional Animal Care and Use Committee (CEUA 113/16) to ensure compliance with ethical standards.

ENU mutagenesis, breeding, and genotyping

The ENU mutagenesis, breeding, and genotyping procedures have been previously described (*17*). In summary, C57BL/6J male mice were subjected to ENU mutagenesis (referred to as G0 mice) and subsequently mated with C57BL/6J females to produce G1 males carrying the mutations. The entire exomes of all G1 mice were sequenced to identify ENU-induced alleles. Among them, G1 males harboring 30 or more mutations in coding regions or splicing sites were considered as founders and were bred with C57BL/6J females, resulting in G2 females carrying the mutations.

To maintain the mutations, the G2 females were backcrossed with their G1 fathers. High-throughput target capture sequencing was performed to genotype both the G2 females and the resulting G3 offspring. This comprehensive pipeline allows for the generation of 30 to 100 G3 mice per pedigree, each carrying all the identified mutations in either homozygous or heterozygous states. This approach ensures accurate identification and clear lineage tracing for each mouse in the pedigree.

BP and HR screening

We used a noninvasive screening method using tail cuff plethysmography (BP-2000 Blood Pressure Analysis System for Mice, Visitech Systems Inc.) to measure SBP and HR in conscious mice. All mice of the G3 pedigree, spanning ages from 50 to 250 days, were registered collectively in a single batch. Age-matched WT animals were screened together with G3 mice, and normalization was performed relative to the screening results of the WT controls. Each mouse was gently secured in an animal holder for a duration of 20 min, and its tail was positioned to accommodate a cuff and sensor for SBP/HR measurement.

To ensure the animals' comfort and familiarization, five preliminary assessments were conducted on each experiment day before obtaining the final results. Subsequently, an additional 10 automated assessments were performed at 15-s intervals, and the average value was recorded as the measurement for that day. This entire procedure was repeated for three consecutive days, wherein the data from the initial day were disregarded as it served solely for training purposes and was not included in the analysis.

AMM of ENU alleles

The SBP/HR values obtained from days 2 and 3 were used to calculate average SBP and HR values, enabling automated mapping of ENU alleles. Automated genetic mapping for monogenic traits was conducted following a previously described protocol (*17*). In summary, the analysis involved automated computational linkage analysis for each mutation in a pedigree using recessive, additive, or dominant models of transmission, employing the Linkage Analyzer software. To examine the relationship between the quantitative phenotype and genotype (REF: homozygous for reference allele; HET: heterozygous for reference and variant allele; VAR: homozygous for variant allele) at each mutation in all mice within the pedigree, a generalized linear mixed model was used. Maternal information was treated as a random effect variable in the analysis. For each gene, a likelihood ratio test derived from the generalized linear mixed model was used to evaluate the association between numerical genotypes and BP and HR, with adjustments made for G3 mouse gender. The resulting *P* values were corrected using the Bonferroni procedure.

We investigated the necessity of adjusting models for age and body weight, in addition to gender, since these covariates are commonly used in BP association studies in human populations. To this end, we evaluated the impact of these covariates on SBP using a generalized linear model, analyzing data from the first 10 phenotyped experimental groups of C57BL/6J control mice. Furthermore, we monitored 10 C57BL/6J control mice (comprising four females and six males) from the 6th to the 37th week of age, using a linear mixed model to determine the influence of age, gender, and weight on SBP, treating individual animals as a random effect. Our analysis revealed that age and weight did not significantly affect SBP values in either analysis (*P* values of >0.05 in both linear and linear mixed models).

The criteria for candidate declaration included at least two homozygous mice for each implicated mutation site, a pedigree size of at least 20 mice, and a *P* value of <0.05 with Bonferroni correction testing the null hypothesis of non-association between mutation and phenotype in any of three inheritance models (dominant, additive, or recessive), according to both raw and normalized averages of data from the 2 days of phenotyping (Fig. 1A).

Detecting lethal effects

The probability of a gene being lethal when disrupted was estimated using a model trained on the known functions of seven essential genes. In addition, the likelihood of encountering equally rare or rarer G3 mice with VAR genotypes was determined using Fisher's exact test. This assessment also incorporated data on the essentiality of corresponding human orthologs, as derived from cell line studies and population genetics.

Candidate Explorer

CE is an advanced supervised machine learning tool designed to enhance the identification of mutations that play a causal role in screened phenotypes and are promising candidates for future studies involving engineered mice (*22*). By integrating 67 distinct features into a unified numeric score, CE effectively evaluates the mutations and classifies them into categorical assessments, including "excellent candidate," "good candidate," "potential candidate," and "not good candidate."

To train CE, a comprehensive dataset comprising verified and excluded mutation-phenotype associations is used. These associations are established through germline retargeting techniques using CRISPR-Cas9 KO or replacement alleles, with the latter applied in cases involving homozygous lethality. CE leverages diverse input data, such as phenotype, linkage, mutation, and gene features assessed in the Beutler laboratory. Notably, it incorporates measures like phenotypic overlap between genotypes, phenotypic overlap between VAR mice and C57BL/6J control mice, magnitude of phenotypic effect between genotypes, phenotypic variance between genotypes, and mutation classification by Polyphen2 and Sift algorithms.

Regarding the classification of BP and HR genes identified by AMM, the CE results from November 2022 were used. These results serve as a valuable resource for the categorization and prioritization of these genes in the context of their potential causal roles and suitability for further investigation.

Literature evidences

To identify candidate genes associated with BP and HR phenotypes, we conducted a thorough investigation using multiple reliable sources of information. First, we extensively searched the National Center for Biotechnology Information (NCBI) database at https://ncbi.nlm.nih.gov/ to explore the functional aspects of genes related to these phenotypes. In addition, we thoroughly reviewed the scientific literature for evidence supporting their impact on BP and HR. To ensure a comprehensive analysis, we used Pharos, an upstream literature-based tool available at https://pharos.nih.gov/, to gather further insights. Moreover, we extended our investigation to the ClinVar database, accessible at https://ncbi.nlm.nih.gov/clinvar/. This allowed us to examine genetic variations within our candidate genes that have been linked to various human syndromes and conditions. By incorporating these diverse resources, we aimed to distinguish the candidate genes associated with BP and HR phenotypes and gain a comprehensive understanding of their functional relevance, documented evidence, and potential genetic variations related to human health conditions.

Validation of candidate genes with reverse genetics

Generation of KO mice

We used the CRISPR Design tool (https://chopchop.cbu.uib.no/) to select target sites for CRISPR editing in five candidate genes (*Duox2*, *Zfp106*, *Kl*, *Notch3*, and *Nae1*). The corresponding CRISPR guide RNAs were synthesized as previously described (*17*). The microinjection technique was used to introduce CRISPR components into zygotes for precise gene targeting, following an established protocol (*17*). Initially, female C57BL/6J mice were super-ovulated and then mated with C57BL/6JJcl male mice (obtained from The Jackson Laboratory) overnight. Fertilized eggs were collected from the oviducts the next day, and *Cas9* mRNA and guide RNA were in vitro transcribed and injected into the pronucleus or cytoplasm of the fertilized eggs. To generate mutant mice, two-cell stage embryos were transferred to pseudo-pregnant Hsd:CR (CD-1) females (sourced from Harlan Laboratory).

Tail samples were obtained from the surviving mice (C1) for DNA extraction and subsequent genotyping through sequencing. By analyzing the genetic alterations, including frameshift mutations, stop loss, or stop gain, we identified mice carrying heterozygous or homozygous mutations, resulting in modified or absent protein expression. Heterozygous C1 mice were then bred with C57BL/6J mice to obtain C2 mice with heterozygous mutations. Subsequent mating between these C2 mice allowed us to generate C3 progeny, encompassing WT, heterozygous, and homozygous mutant mice for further evaluation of phenotypic traits using plethysmography.

Target genes KO mice phenotype confirmation by plethysmography

The BP differences between KO and WT mice were evaluated using a noninvasive method to measure tail cuff BP in conscious mice, which was the same method used in the G3 phenotypic screening using the BP-2000 Blood Pressure Analysis System for Mice, developed by Visitech Systems Inc. Homozygous KO, heterozygous, and WT mice from the same progeny were included in the study. During the validation phase, animals were registered for three consecutive days. Similar to the initial screening, data from the first day were considered as training data and disregarded. To assess the SBP/HR differences between mutations, genotypes, and gender, a three-way analysis of variance (ANOVA) with an interaction term was performed. Bonferroni post tests were conducted on the average SBP/HR values obtained from 2 days. In cases where only one mutated strain was developed, a two-way ANOVA with an interaction term was used to assess the SBP/HR differences between genotypes and gender.

Enrichment of candidate genes nearby BP and HR significant GWAS loci

Our study involved a detailed association analysis to understand the relationship between genetic variants in or near candidate genes and BP or HR traits in humans. This analysis was conducted using the GWAS catalog database (https://ebi.ac.uk/gwas/, version 1.0.3, accessed on 29 October 2023). We focused on studies linked to BP and HR traits, specifically those containing keywords like HR, atrial fibrillation, various medication usages (e.g., beta blockers, calcium channel blockers, and diuretics), and electrocardiographic traits. Our aim was to determine whether our candidate genes showed significant enrichment near SNPs identified in GWAS studies for these traits. This was assessed using the hypergeometric test, employing the phyper function in R. The analysis was confined to coding genes within the human genome (GRCh38, from Ensemble release 110) and the BP- and HR-related trait entries from the GWAS catalog.

Supplementary Materials

This PDF file includes:

Figs. S1 to S4
Legends for tables S1 to S5
Table S6
Legends for tables S7 to S9
References

Other Supplementary Material for this manuscript includes the following:

Tables S1 to S5 and S7 to S9

REFERENCES AND NOTES

1. WHO, *Global Health Risks* (WHO, 2009).
2. A. V. Chobanian, G. L. Bakris, H. R. Black, W. C. Cushman, L. A. Green, J. L. Izzo Jr., D. W. Jones, B. J. Materson, S. Oparil, J. T. Wright Jr., E. J. Roccella; National Heart, Lung, and Blood Institute Joint National Committee on Prevention, Detection, Evaluation, and Treatment of High Blood Pressure; National High Blood Pressure Education Program Coordinating Committee, The Seventh Report of the Joint National Committee on Prevention, Detection, Evaluation, and Treatment of High Blood Pressure: The JNC 7 report. *JAMA* **289**, 2560–2572 (2003).
3. I. Hajjar, T. A. Kotchen, Trends in prevalence, awareness, treatment, and control of hypertension in the United States, 1988–2000. *JAMA* **290**, 199–206 (2003).
4. P. M. Kearney, M. Whelton, K. Reynolds, P. Muntner, P. K. Whelton, J. He, Global burden of hypertension: Analysis of worldwide data. *Lancet* **365**, 217–223 (2005).
5. K. Fox, J. S. Borer, A. J. Camm, N. Danchin, R. Ferrari, J. L. Lopez Sendon, P. G. Steg, J. C. Tardif, L. Tavazzi, M. Tendera, Resting heart rate in cardiovascular disease. *J. Am. Coll. Cardiol.* **50**, 823–830 (2007).
6. P. Greenland, M. L. Daviglus, A. R. Dyer, K. Liu, C. F. Huang, J. J. Goldberger, J. Stamler, Resting heart rate is a risk factor for cardiovascular and noncardiovascular mortality: The Chicago Heart Association Detection Project in Industry. *Am. J. Epidemiol.* **149**, 853–862 (1999).
7. P. Palatini, Elevated resting heart rate is a risk factor for sudden death in middle-aged men. *Evid. Based Cardiovasc. Med.* **5**, 86 (2001).
8. C. M. de Oliveira, A. C. Pereira, M. de Andrade, J. M. Soler, J. E. Krieger, Heritability of cardiovascular risk factors in a Brazilian population: Baependi Heart Study. *BMC Med. Genet.* **9**, 32 (2008).
9. G. B. Ehret, Genome-wide association studies: Contribution of genomics to understanding blood pressure and essential hypertension. *Curr. Hypertens. Rep.* **12**, 17–25 (2010).
10. J. P. Singh, M. G. Larson, C. J. O'Donnell, H. Tsuji, J. C. Evans, D. Levy, Heritability of heart rate variability: The framingham heart study. *Circulation* **99**, 2251–2254 (1999).
11. C. Newton-Cheh, M. G. Larson, D. C. Corey, E. J. Benjamin, A. G. Herbert, D. Levy, R. B. D'Agostino, C. J. O'Donnell, QT interval is a heritable quantitative trait with evidence of linkage to chromosome 3 in a genome-wide linkage analysis: The Framingham Heart Study. *Hear. Rhythm* **2**, 277–284 (2005).
12. C. Newton-Cheh, C.-Y. Guo, T. J. Wang, C. J. O'Donnell, D. Levy, M. G. Larson, Genome-wide association study of electrocardiographic and heart rate variability traits: The Framingham Heart Study. *BMC Med. Genet.* **8**, S7 (2007).
13. S. Padmanabhan, B. Joe, Towards precision medicine for hypertension: A review of genomic, epigenomic, and microbiomic effects on blood pressure in experimental rat models and humans. *Physiol. Rev.* **97**, 1469–1528 (2017).
14. E. Evangelou, H. R. Warren, D. Mosen-Ansorena, B. Mifsud, R. Pazoki, H. Gao, G. Ntritsos, N. Dimou, C. P. Cabrera, I. Karaman, F. L. Ng, M. Evangelou, K. Witkowska, E. Tzanis, J. N. Hellwege, A. Giri, D. R. V. Edwards, Y. V. Sun, K. Cho, J. M. Gaziano, P. W. F. Wilson, P. S. Tsao, C. P. Kovesdy, T. Esko, R. Magi, L. Milani, P. Almgren, T. Boutin, S. Debette, J. Ding, F. Giulianini, E. G. Holliday, A. U. Jackson, R. Li-Gao, W.-Y. Lin, J. Luan, M. Mangino, C. Oldmeadow, B. Prins, Y. Qian, M. Sargurupremraj, N. Shah, P. Surendran, S. Theriault, N. Verweij, S. M. Willems, J.-H. Zhao, P. Amouyel, J. Connell, R. de Mutsert, A. S. F. Doney, M. Farrall, C. Menni, A. D. Morris, R. Noordam, G. Pare, N. R. Poulter, D. C. Shields, A. Stanton, S. Thom, G. Abecasis, N. Amin, D. E. Arking, K. L. Ayers, C. M. Barbieri, C. Batini, J. C. Bis, T. Blake, M. Bochud, M. Boehnke, E. Boerwinkle, D. I. Boomsma, E. Bottinger, P. S. Braund, M. Brumat, A. Campbell, H. Campbell, A. Chakravarti, J. C. Chambers, G. Chauhan, M. Ciullo, M. Cocca, F. Collins, H. J. Cordell, G. Davies, M. H. de Borst, E. de Geus, I. Deary, J. Deelen, F. M. Del Greco, C. Y. Demirkale, M. Dorr, G. B. Ehret, R. Elosua, S. Enroth, A. M. Erzurumluoglu, T. Ferreira, M. Franberg, O. H. Franco, I. Gandin, P. Gasparini, V. Giedraitis, C. Gieger, G. Girotto, A. Goel, A. J. Gow, V. Gudnason, X. Guo, U. Gyllensten, A. Hamsten, T. B. Harris, S. E. Harris, C. A. Hartman, A. S. Havulinna, A. A. Hicks, E. Hofer, A. Hofman, J.-J. Hottenga, J. E. Huffman, S.-J. Hwang, E. Ingelsson, A. James, R. Jansen, M.-R. Jarvelin, R. Joehanes, A. Johansson, A. D. Johnson, P. Joshi, P. Jousilahti, J. W. Jukema, A. M. Jula, M. Kahonen, S. Kathiresan, B. D. Keavney, K.-T. Khaw, P. Knekt, J. Knight, I. Kolcic, J. S. Kooner, S. Koskinen, K. Kristiansson, Z. Kutalik, M. Laan, M. Larson, L. J. Launer, B. Lehne, T. Lehtimaki, D. Levy, D. C. M. Liewald, L. Lin, L. Lind, C. M. Lindgren, Y. Liu, R. J. F. Loos, L. M. Lopez, L. Lu, L.-P. Lyytikainen, A. Mahajan, C. Mamasoula, J. Marrugat, J. Marten, Y. Milaneschi, A. Morgan, A. P. Morris, A. C. Morrison, M. A. Nalls, P. Nandakumar, C. P. Nelson, C. Newton-Cheh, T. Niiranen, I. M. Nolte, T. Nutile, A. J. Oldehinkel, B. A. Oostra, P. F. O'Reilly, E. Org, S. Padmanabhan, W. Palmas, A. Palotie, A. Pattie, B. W. J. H. Penninx, M. Perola, P. J. Munson, A. Peters, O. Polasek, P. P. Pramstaller, N. Q. Tri, O. T. Raitakari, M. Ren, R. Rettig, K. Rice, P. M. Ridker, J. S. Reid, H. Riese, S. Ripatti, A. Robino, L. M. Rose, J. I. Rotter, I. Rudan, D. Ruggiero, Y. Saba, C. F. Sala, V. Salomaa, N. J. Samani, A.-P. Sarin, R. Schmidt, H. Schmidt, N. Shrine, D. Siscovick, A. V. Smith, H. Schneider, S. Sober, R. Sorice, J. M. Starr, D. J. Stott, D. P. Strachan, R. J. Strawbridge, J. Sundstrom, M. A. Swertz, K. D. Taylor, A. Teumer, M. D. Tobin, D. Toniolo, M. Traglia, S. Trompet, J. Tuomilehto, C. Tzourio, A. G. Uitterlinden, A. Vaez, P. J. van der Most, C. M. van Duijn, A.-C. Vergnaud, G. C. Verwoert, V. Vitart, U. Volker, P. Vollenweider, D. Vuckovic, H. Watkins, S. H. Wild, G. Willemsen, J. F. Wilson, A. F. Wright, J. Yao, T. Zemunik, W. Zhang, J. R. Attia, A. S. Butterworth, D. I. Chasman, D. Conen, F. Cucca, J. Danesh, C. Hayward, J. M. M. Howson, M. Laakso, E. G. Lakatta, C. Langenberg, O. Melander, D. O. Mook-Kanamori, P. B. Munroe, C. N. A. Palmer, L. Risch, R. A. Scott, R. J. Scott, P. Sever, T. D. Spector, P. van der Harst, N. J. Wareham, E. Zeggini, M. J. Brown, A. Metspalu, A. M. Hung, C. O'Donnell, T. L. Edwards, B. M. Psaty, I. Tzoulaki, M. R. Barnes, L. V. Wain, P. Elliott, M. J. Caulfield, Genetic analysis of over 1 million people identifies 535 new loci associated with blood pressure traits. *Nat. Genet.* **50**, 1412–1425 (2018).
15. R. N. Eppinga, Y. Hagemeijer, S. Burgess, D. A. Hinds, K. Stefansson, D. F. Gudbjartsson, D. J. Van Veldhuisen, P. B. Munroe, N. Verweij, P. Van Der Harst, Identification of genomic loci associated with resting heart rate and shared genetic predictors with all-cause mortality. *Nat. Genet.* **48**, 1557–1563 (2016).
16. K. R. Bull, A. J. Rimmer, O. M. Siggs, L. A. Miosge, C. M. Roots, A. Enders, E. M. Bertram, T. L. Crockford, B. Whittle, P. K. Potter, M. M. Simon, A. M. Mallon, S. D. M. Brown, B. Beutler,

C. C. Goodnow, G. Lunter, R. J. Cornall, Unlocking the bottleneck in forward genetics using whole-genome sequencing and identity by descent to isolate causative mutations. *PLOS Genet.* **9**, e1003219 (2013).
17. T. Wang, X. Zhan, C.-H. Bu, S. Lyon, D. Pratt, S. Hildebrand, J. H. Choi, Z. Zhang, M. Zeng, K. Wang, E. Turer, Z. Chen, D. Zhang, T. Yue, Y. Wang, H. Shi, J. Wang, L. Sun, J. SoRelle, W. McAlpine, N. Hutchins, X. Zhan, M. Fina, R. Gobert, J. Quan, M. Kreutzer, S. Arnett, K. Hawkins, A. Leach, C. Tate, C. Daniel, C. Reyna, L. Prince, S. Davis, J. Purrington, R. Bearden, J. Weatherly, D. White, J. Russell, Q. Sun, M. Tang, X. Li, L. Scott, E. M. Y. Moresco, G. M. McInerney, G. B. Karlsson Hedestam, Y. Xie, B. Beutler, Real-time resolution of point mutations that cause phenovariance in mice. *Proc. Natl. Acad. Sci. U.S.A.* **112**, E440–E449 (2015).
18. P. M. Nolan, J. Peters, M. Strivens, D. Rogers, J. Hagan, N. Spurr, I. C. Gray, L. Vizor, D. Brooker, E. Whitehill, R. Washbourne, T. Hough, S. Greenaway, M. Hewitt, X. Liu, S. McCormack, K. Pickford, R. Selley, C. Wells, Z. Tymowska-Lalanne, P. Roby, P. Glenister, C. Thornton, C. Thaung, J. A. Stevenson, R. Arkell, P. Mburu, R. Hardisty, A. Kiernan, A. Erven, K. P. Steel, S. Voegeling, J. L. Guenet, C. Nickols, R. Sadri, M. Nasse, A. Isaacs, K. Davies, M. Browne, E. M. Fisher, J. Martin, S. Rastan, S. D. Brown, J. Hunter, A systematic, genome-wide, phenotype-driven mutagenesis programme for gene function studies in the mouse. *Nat. Genet.* **25**, 440–443 (2000).
19. M. H. De Angelis, H. Flaswinkel, H. Fuchs, B. Rathkolb, D. Soewarto, S. Marschall, S. Heffner, W. Pargent, K. Wuensch, M. Jung, A. Reis, T. Richter, F. Alessandrini, T. Jakob, E. Fuchs, H. Kolb, E. Kremmer, K. Schaeble, B. Rollinski, A. Roscher, C. Peters, T. Meitinger, T. Strom, T. Steckler, F. Holsboer, T. Klopstock, F. Gekeler, C. Schindewolf, T. Jung, K. Avraham, H. Behrendt, J. Ring, A. Zimmer, K. Schughart, K. Pfeffer, E. Wolf, R. Balling, Genome-wide, large-scale production of mutant mice by ENU mutagenesis. *Nat. Genet.* **25**, 444–447 (2000).
20. P. Haffter, M. Granato, M. Brand, M. C. Mullins, M. Hammerschmidt, D. A. Kane, J. Odenthal, F. J. M. Van Eeden, Y. J. Jiang, C. P. Heisenberg, R. N. Kelsh, M. Furutani-Seiki, E. Vogelsang, D. Beuchle, U. Schach, C. Fabian, C. Nüsslein-Volhard, The identification of genes with unique and essential functions in the development of the zebrafish, *Danio rerio*. *Development* **123**, 1–36 (1996).
21. M. M. Simon, E. M. Y. Moresco, K. R. Bull, S. Kumar, A.-M. Mallon, B. Beutler, P. K. Potter, Current strategies for mutation detection in phenotype-driven screens utilising next generation sequencing. *Mamm. Genome* **26**, 486–500 (2015).
22. D. Xu, S. Lyon, C. H. Bu, S. Hildebrand, J. H. Choi, X. Zhong, A. Liu, E. E. Turer, Z. Zhang, J. Russell, S. Ludwig, E. Mahrt, E. Nair-Gill, H. Shi, Y. Wang, D. Zhang, T. Yue, K. W. Wang, J. A. SoRelle, L. Su, T. Misawa, W. McAlpine, L. Sun, J. Wang, X. Zhan, M. Choi, R. Farokhnia, A. Sakla, S. Schneider, H. Coco, G. Coolbaugh, B. Hayse, S. Mazal, D. Medler, B. Nguyen, E. Rodriguez, A. Wadley, M. Tang, X. Li, P. Anderton, K. Keller, A. Press, L. Scott, J. Quan, S. Cooper, T. Collie, B. Qin, J. Cardin, R. Simpson, M. Tadesse, Q. Sun, C. A. Wise, J. J. Rios, E. M. Y. Moresco, B. Beutler, Thousands of induced germline mutations affecting immune cells identified by automated meiotic mapping coupled with machine learning. *Proc. Natl. Acad. Sci. U.S.A.* **118**, e2106786118 (2021).
23. T. Wang, C. H. Bu, S. Hildebrand, G. Jia, O. M. Siggs, S. Lyon, D. Pratt, L. Scott, J. Russell, S. Ludwig, A. R. Murray, E. M. Y. Moresco, B. Beutler, Probability of phenotypically detectable protein damage by ENU-induced mutations in the Mutagenetix database. *Nat. Commun.* **9**, 441 (2018).
24. J. Lu, X. Hou, X. Yuan, L. Cui, Z. Liu, X. Li, L. Ma, X. Cheng, Y. Xin, C. Wang, K. Zhang, X. Wang, W. Ren, R. Sun, Z. Jia, Z. Tian, Q. S. Mi, C. Li, Knockout of the urate oxidase gene provides a stable mouse model of hyperuricemia associated with metabolic disorders. *Kidney Int.* **93**, 69–80 (2018).
25. J. Greenfield, J. Greenfield, J. Miller, J. Miller, J. Keogh, J. Keogh, E. Henning, E. Henning, J. Satterwhite, J. Satterwhite, G. Cameron, G. Cameron, B. Astruc, B. Astruc, J. Mayer, J. Mayer, S. Brage, S. Brage, T. See, T. See, D. Lomas, D. Lomas, S. O'Rahilly, S. O'Rahilly, I. Farooqi, I. Farooqi, Modulation of blood pressure by central melanocortinergic pathways. *N. Engl. J. Med.* **360**, 44–52 (2009).
26. J. M. do Carmo, A. A. da Silva, Z. Wang, T. Fang, N. Aberdein, C. E. P. de Lara, J. E. Hall, Role of the brain melanocortins in blood pressure regulation. *Biochim. Biophys. Acta Mol. Basis Dis.* **1863**, 2508–2514 (2017).
27. A. L. Mark, R. A. Shaffer, M. L. Correia, D. A. Morgan, C. D. Sigmund, W. G. Haynes, Contrasting blood pressure effects of obesity in leptin-deficient ob/ob mice and agouti yellow obese mice. *J. Hypertens.* **17**, 1949–1953 (1999).
28. J. J. Kuo, A. A. Silva, J. E. Hall, Hypothalamic melanocortin receptors and chronic regulation of arterial pressure and renal function. *Hypertension* **41**, 768–774 (2003).
29. R. E. Pyeritz, V. A. McKusick, The Marfan syndrome: Diagnosis and management. *N. Engl. J. Med.* **300**, 772–777 (1979).
30. M. A. Baum, H. W. Harris, P. E. Burrows, D. E. Schofield, M. J. G. Somers, Renovascular hypertension in Marfan syndrome. *Pediatr. Nephrol.* **11**, 499–501 (1997).
31. J. Jeppesen, N. D. Berg, C. Torp-Pedersen, T. W. Hansen, A. Linneberg, M. Fenger, Fibrillin-1 genotype and risk of prevalent hypertension: A study in two independent populations. *Blood Press.* **21**, 273–280 (2012).
32. A. Cherkas, R. Zhuraev, A marked decrease in heart rate variability in Marfan syndrome patients with confirmed FBN1 mutations. *Cardiol. J.* **23**, 23–33 (2016).
33. P. Peres, A. C. Carvalho, A. B. A. Perez, W. M. Medeiros, Abnormal heart rate recovery and deficient chronotropic response after submaximal exercise in young Marfan syndrome patients. *Cardiol. Young* **26**, 1274–1281 (2016).
34. S. R. F. Twigg, D. Lloyd, D. Jenkins, N. E. Elçioglu, C. D. O. Cooper, N. Al-Sannaa, A. Annagür, G. Gillessen-Kaesbach, I. Hüning, S. J. L. Knight, J. A. Goodship, B. D. Keavney, P. L. Beales, O. Gileadi, S. J. McGowan, A. O. M. Wilkie, Mutations in multidomain protein MEGF8 identify a carpenter syndrome subtype associated with defective lateralization. *Am. J. Hum. Genet.* **91**, 897–905 (2012).
35. J. J. Johnston, J. J. van der Smagt, J. A. Rosenfeld, A. T. Pagnamenta, A. Alswaid, E. H. Baker, E. Blair, G. Borck, J. Brinkmann, W. Craigen, V. C. Dung, L. Emrick, D. B. Everman, K. L. van Gassen, S. Gulsuner, M. H. Harr, M. Jain, A. Kuechler, K. A. Leppig, D. M. McDonald-McGinn, N. T. B. Can, A. Peleg, E. R. Roeder, R. C. Rogers, L. Sagi-Dain, J. C. Sapp, A. A. Schäffer, D. Schanze, H. Stewart, J. C. Taylor, N. E. Verbeek, M. A. Walkiewicz, E. H. Zackai, C. Zweier, M. Zenker, B. Lee, L. G. Biesecker, Autosomal recessive Noonan syndrome associated with biallelic LZTR1 variants. *Genet. Med.* **20**, 1175–1185 (2018).
36. J. Manoochehri, H. R. Goodarzi, S. M. B. Tabei, Spastic paraplegia 51: Phenotypic spectrum related to novel homozygous *AP4E1* mutation. *J. Genet.* **101**, 1–6 (2022).
37. N. Spielmann, G. Miller, T. I. Oprea, C.-W. Hsu, G. Fobo, G. Frishman, C. Montrone, H. H. Mashhadi, J. Mason, V. M. Fuentes, S. Leuchtenberger, A. Ruepp, M. Wagner, D. S. Westphal, C. Wolf, A. Görlach, A. Sanz-Moreno, Y.-L. Cho, R. Teperino, S. Brandmaier, S. Sharma, I. R. Galter, M. A. Östereicher, L. Zapf, P. Mayer-Kuckuk, J. Rozman, L. Teboul, R. K. A. Bunton-Stasyshyn, H. Cater, M. Stewart, S. Christou, H. Westerberg, A. M. Willett, J. M. Wotton, W. B. Roper, A. E. Christiansen, C. S. Ward, J. D. Heaney, C. L. Reynolds, J. Prochazka, L. Bower, D. Clary, M. Selloum, G. B. About, O. Wendling, H. Jacobs, S. Leblanc, H. Meziane, T. Sorg, E. Audain, A. Gilly, N. W. Rayner, J. A. Aguilar-Pimentel, L. Becker, L. Garrett, S. M. Hölter, O. V. Amarie, J. Calzada-Wack, T. Klein-Rodewald, P. da Silva-Buttkus, C. Lengger, C. Stoeger, R. Gerlini, B. Rathkolb, D. Mayr, J. Seavitt, A. Gaspero, J. R. Green, A. Garza, R. Bohat, L. Wong, M. L. McElwee, S. Kalaga, T. L. Rasmussen, I. Lorenzo, D. G. Lanza, R. C. Samaco, S. Veeraragaven, J. J. Gallegos, P. Kašpárek, S. Petrezsélyová, R. King, S. Johnson, J. Cleak, Z. Szkoe-Kovacs, G. Codner, M. Mackenzie, A. Caulder, J. Kenyon, W. Gardiner, H. Phelps, R. Hancock, C. Norris, M. A. Moore, A. M. Seluke, R. Urban, C. Kane, L. O. Goodwin, K. A. Peterson, M. Mckay, J. J. Cook, J. P. Lowy, M. McFarland, J. A. Wood, B. J. Willis, H. Tolentino, T. Tolentino, M. Schuchbauer, J. Salazar, J. Johnson, R. Munson, A. Ayadi, G. Pavlovic, M.-C. Birling, S. Jacquot, D. Ali-Hadji, P. Charles, P. Andre, M.-F. Champy, F. Riet, I. Vukobradovic, Z. Berberovic, D. Qu, R. Guo, A. D'Souza, Z. Huang, S. Camilleri, M. Ganguly, H. Adissu, M. Eskandarian, X. Shang, K. Duffin, C. Xu, K. Roberton, V. Laurin, Q. Lan, G. Sleep, A. Creighton, L. Lintott, M. Gertsenstein, M. Pereira, S. Tondat, A. Patel, M. Cruz, A. Bezginov, D. Miller, W. Hy, A. Yoshiki, N. Tanaka, M. Tamura, Z. Liu, O. Ermakova, A. Ferrara, P. Fruscoloni, C. Seisenberger, A. Bürger, F. Giesert, J. C. Ambrose, P. Arumu Gam, R. Bevers, M. Bleda, F. Boardman-Pretty, C. R. Boustred, H. Brittain, M. J. Caulfield, G. C. Chan, T. Fowler, A. Giess, A. Hamblin, S. Henderson, T. J. P. Hubbard, R. Jackson, L. J. Jones, D. Kasperaviciute, M. Kayikci, A. Kousathanas, L. Lahnstein, S. E. A. Leigh, I. U. S. Leong, F. J. Lopez, F. Maleady-Crowe, M. McEntagart, F. Minneci, L. Moutsianas, M. Mueller, N. Murugaesu, A. C. Need, P. O'Donovan, C. A. Odhams, C. Patch, D. Perez-Gil, M. B. Pereira, J. Pullinger, T. Rahim, A. Rendon, T. Rogers, K. Savage, K. Sawant, R. H. Scott, A. Siddiq, A. Sieghart, S. C. Smith, A. Sosinsky, A. Stuckey, M. Tanguy, A. L. Taylor-Tavares, E. R. A. Thomas, S. R. Thompson, A. Tucci, M. J. Welland, E. Williams, K. Witkowska, S. M. Wood, M.-P. Hitz, E. Zeggini, E. Wolf, R. Sedlacek, S. A. Murray, K. L. Svenson, R. E. Braun, J. K. White, L. Kelsey, X. Gao, T. Shiroishi, Y. Xu, J. K. Seong, F. Mammano, G. P. Tocchini-Valentini, A. L. Beaudet, T. F. Meehan, H. Parkinson, D. Smedley, A.-M. Mallon, S. E. Wells, H. Grallert, W. Wurst, S. Marschall, H. Fuchs, S. D. M. Brown, A. M. Flenniken, L. M. J. Nutter, C. McKerlie, Y. Herault, K. C. K. Lloyd, M. E. Dickinson, V. Gailus-Durner, M. H. de Angelis, Extensive identification of genes involved in congenital and structural heart disorders and cardiomyopathy. *Nat. Cardiovasc. Res.* **1**, 157–173 (2022).
38. J. O. Szot, H. Cuny, G. M. Blue, D. T. Humphreys, E. Ip, K. Harrison, G. F. Sholler, E. Giannoulatou, P. Leo, E. L. Duncan, D. B. Sparrow, J. W. K. Ho, R. M. Graham, N. Pachter, G. Chapman, D. S. Winlaw, S. L. Dunwoodie, A screening approach to identify clinically actionable variants causing congenital heart disease in exome data. *Circ. Genomic Precis. Med.* **11**, e001978 (2018).
39. I. J. J. Muffels, I. F. Schene, H. Rehmann, M. P. G. Massink, M. M. van der Wal, C. Bauder, M. Labeur, N. G. Armando, M. H. Lequin, M. L. Houben, J. C. Giltay, S. Haitjema, A. Huisman, F. Vansenne, J. Bluvstein, J. Pappas, L. V. Shailee, Y. A. Zarate, M. Mokry, G. W. van Haaften, P. M. van Hasselt, Bi-allelic variants in NAE1 cause intellectual disability, ischiopubic hypoplasia, stress-mediated lymphopenia and neurodegeneration. *Am. J. Hum. Genet.* **110**, 146–160 (2023).
40. S. Kandala, I. M. Kim, H. Su, Neddylation and deneddylation in cardiac biology. *Am. J. Cardiovasc. Dis.* **4**, 140–158 (2014).
41. J. Zou, W. Ma, J. Li, R. Littlejohn, H. Zhou, I. I.-M. Kim, D. J. R. Fulton, W. Chen, N. L. Weintraub, J. Zhou, H. Su, Neddylation mediates ventricular chamber maturation

through repression of Hippo signaling. *Proc. Natl. Acad. Sci. U.S.A.* **115**, E4101–E4110 (2018).
42. T. Kamitani, K. Kito, H. P. Nguyen, E. T. H. Yeh, Characterization of NEDD8, a developmentally down-regulated ubiquitin-like protein. *J. Biol. Chem.* **272**, 28557–28562 (1997).
43. J. Zou, W. Ma, R. Littlejohn, J. Li, B. K. Stansfield, I. M. Kim, J. Liu, J. Zhou, N. L. Weintraub, H. Su, Transient inhibition of neddylation at neonatal stage evokes reversible cardiomyopathy and predisposes the heart to isoproterenol-induced heart failure. *Am. J. Physiol. Heart Circ. Physiol.* **316**, H1406–H1416 (2019).
44. J. C. Moreno, H. Bikker, M. J. E. Kempers, A. S. P. van Trotsenburg, F. Baas, J. J. M. de Vijlder, T. Vulsma, C. Ris-Stalpers, Inactivating mutations in the gene for thyroid oxidase 2 (THOX2) and congenital hypothyroidism. *N. Engl. J. Med.* **347**, 95–102 (2002).
45. S. Danzi, I. Klein, Thyroid hormone and blood pressure regulation. *Curr. Hypertens. Rep.* **5**, 513–520 (2003).
46. J. J. Rios, K. Denton, J. Russell, J. Kozlitina, C. R. Ferreira, A. F. Lewanda, J. E. Mayfield, E. Moresco, S. Ludwig, M. Tang, X. Li, S. Lyon, A. Khanshour, N. Paria, A. Khalid, Y. Li, X. Xie, J. Q. Feng, Q. Xu, Y. Lu, R. E. Hammer, C. A. Wise, B. Beutler, Germline saturation mutagenesis induces skeletal phenotypes in mice. *J. Bone Miner. Res.* **36**, 1548–1565 (2021).
47. D. M. Anderson, J. Cannavino, H. Li, K. M. Anderson, B. R. Nelson, J. McAnally, S. Bezprozvannaya, Y. Liu, W. Lin, N. Liu, R. Bassel-Duby, E. N. Olson, Severe muscle wasting and denervation in mice lacking the RNA-binding protein ZFP106. *Proc. Natl. Acad. Sci. U.S.A.* **113**, E4494–E4503 (2016).
48. M. Kuro-o, Y. Matsumura, H. Aizawa, H. Kawaguchi, T. Suga, T. Utsugi, Y. Ohyama, M. Kurabayashi, T. Kaname, E. Kume, H. Iwasaki, A. Iida, T. Shiraki-Iida, S. Nishikawa, R. Nagai, Y. I. Nabeshima, Mutation of the mouse klotho gene leads to a syndrome resembling ageing. *Nature* **390**, 45–51 (1997).
49. Y. Xu, Z. Sun, Molecular basis of Klotho: From gene to function in aging. *Endocr. Rev.* **36**, 174–193 (2015).
50. O. Andrukhova, U. Zeitz, R. Goetz, M. Mohammadi, B. Lanske, R. G. Erben, FGF23 acts directly on renal proximal tubules to induce phosphaturia through activation of the ERK1/2-SGK1 signaling pathway. *Bone* **51**, 621–628 (2012).
51. O. Andrukhova, S. Slavic, A. Smorodchenko, U. Zeitz, V. Shalhoub, B. Lanske, E. E. Pohl, R. G. Erben, FGF23 regulates renal sodium handling and blood pressure. *EMBO Mol. Med.* **6**, 744–759 (2014).
52. X. Zhou, K. Chen, Y. Wang, M. Schuman, H. Lei, Z. Sun, Antiaging gene Klotho regulates adrenal CYP11B2 expression and aldosterone synthesis. *J. Am. Soc. Nephrol.* **27**, 1765–1776 (2016).
53. L. J. Chen, M. F. Cheng, P. M. Ku, J. T. Cheng, Cerebral Klotho protein as a humoral factor for maintenance of baroreflex. *Horm. Metab. Res.* **47**, 125–132 (2015).
54. K. Takeshita, T. Fujimori, Y. Kurotaki, H. Honjo, H. Tsujikawa, K. Yasui, J. K. Lee, K. Kamiya, K. Kitaichi, K. Yamamoto, M. Ito, T. Kondo, S. Iino, Y. Inden, M. Hirai, T. Murohara, I. Kodama, Y. I. Nabeshima, Sinoatrial node dysfunction and early unexpected death of mice with a defect of Klotho gene expression. *Circulation* **109**, 1776–1782 (2004).
55. S. Artavanis-Tsakonas, M. D. Rand, R. J. Lake, Notch signaling: Cell fate control and signal integration in development. *Science* **284**, 770–776 (1999).
56. C. Roca, R. H. Adams, Regulation of vascular morphogenesis by Notch signaling. *Genes Dev.* **21**, 2511–2524 (2007).
57. D. Morrow, A. Scheller, Y. A. Birney, C. Sweeney, S. Guha, P. M. Cummins, R. Murphy, D. Walls, E. M. Redmond, P. A. Cahill, Notch-mediated CBF-1/RBP-Jκ-dependent regulation of human vascular smooth muscle cell phenotype in vitro. *Am. J. Physiol. Cell Physiol.* **289**, C1188–C1196 (2005).
58. V. Domenga, P. Fardoux, P. Lacombe, M. Monet, J. Maciazek, L. T. Krebs, B. Klonjkowski, E. Berrou, M. Mericskay, Z. Li, E. Tournier-Lasserve, T. Gridley, A. Joutel, Notch3 is required for arterial identity and maturation of vascular smooth muscle cells. *Genes Dev.* **18**, 2730–2735 (2004).
59. A. Joutel, F. Andreux, S. Gaulis, V. Domenga, M. Cecillon, N. Battail, N. Piga, F. Chapon, C. Godfrain, E. Tournier-Lasserve, The ectodomain of the Notch3 receptor accumulates within the cerebrovasculature of CADASIL patients. *J. Clin. Invest.* **105**, 597–605 (2000).
60. N. Boulos, F. Helle, J.-C. Dussaule, S. Placier, P. Milliez, S. Djudjaj, D. Guerrot, A. Joutel, P. Ronco, J.-J. Boffa, C. Chatziantoniou, Notch3 is essential for regulation of the renal vascular tone. *Hypertension* **57**, 1176–1182 (2011).
61. A. Joutel, C. Corpechot, A. Ducros, K. Vahedit, H. Chabriatt, P. Mouton, S. Alamowitch, V. Domenga, M. Cecillion, E. Marechal, J. Maciazek, C. Vayssiere, C. Cruaud, E.-A. Cabanis, M. Madeleine Ruchoux, J. Weissenbach, J. Fran, O. Bach, M. Germaine Boussert, E. Tournier-Lasserve, Notch3 mutations in CADASIL, a hereditary adult-onset condition causing stroke and dementia. *Nature* **383**, 707–710 (1996).
62. X. Li, X. Zhang, R. Leathers, A. Makino, C. Huang, P. Parsa, J. Macias, J. X. J. Yuan, S. W. Jamieson, P. A. Thistlethwaite, Notch3 signaling promotes the development of pulmonary arterial hypertension. *Nat. Med.* **15**, 1289–1297 (2009).
63. L. T. Krebs, Y. Xue, C. R. Norton, J. P. Sundberg, P. Beatus, U. Lendahl, A. Joutel, T. Gridley, Characterization of Notch3-deficient mice: Normal embryonic development and absence of genetic interactions with a Notch1 mutation. *Genesis* **37**, 139–143 (2003).
64. N. J. Schork, J. E. Krieger, M. R. Trolliet, K. G. Franchini, G. Koike, E. M. Krieger, E. S. Lander, V. J. Dzau, H. J. Jacob, A biometrical genome search in rats reveals the multigenic basis of blood pressure variation. *Genome Res.* **5**, 164–172 (1995).
65. I. Aneas, M. V. Rodrigues, B. A. Pauletti, G. J. J. Silva, R. Carmona, L. Cardoso, A. E. Kwitek, H. J. Jacob, J. M. P. Soler, J. E. Krieger, Congenic strains provide evidence that four mapped loci in chromosomes 2, 4, and 16 influence hypertension in the SHR. *Physiol. Genomics* **37**, 52–57 (2009).
66. R. Kingdom, C. F. Wright, Incomplete penetrance and variable expressivity: From clinical studies to population cohorts. *Front. Genet.* **13**, 1–25 (2022).
67. M. T. Maurano, R. Humbert, E. Rynes, R. E. Thurman, E. Haugen, H. Wang, A. P. Reynolds, R. Sandstrom, H. Qu, J. Brody, A. Shafer, F. Neri, K. Lee, T. Kutyavin, S. Stehling-Sun, A. K. Johnson, T. K. Canfield, E. Giste, M. Diegel, D. Bates, R. S. Hansen, S. Neph, P. J. Sabo, S. Heimfeld, A. Raubitschek, S. Ziegler, C. Cotsapas, N. Sotoodehnia, I. Glass, S. R. Sunyaev, R. Kaul, J. A. Stamatoyannopoulos, Systematic localization of common disease-associated variation in regulatory DNA. *Science* **337**, 1190–1196 (2012).
68. N. R. Wray, C. Wijmenga, P. F. Sullivan, J. Yang, P. M. Visscher, Common disease is more complex than implied by the core gene omnigenic model. *Cell* **173**, 1573–1580 (2018).
69. S. K. Teixeira, A. C. Pereira, J. E. Krieger, Genetics of resistant hypertension: The missing heritability and opportunities. *Curr. Hypertens. Rep.* **20**, 48 (2018).
70. J. Flannick, J. M. Mercader, C. Fuchsberger, M. S. Udler, A. Mahajan, J. Wessel, T. M. Teslovich, L. Caulkins, R. Koesterer, F. Barajas-Olmos, T. W. Blackwell, E. Boerwinkle, J. A. Brody, F. Centeno-Cruz, L. Chen, S. Chen, C. Contreras-Cubas, E. Córdova, A. Correa, M. Cortes, R. A. DeFronzo, L. Dolan, K. L. Drews, A. Elliott, J. S. Floyd, S. Gabriel, M. E. Garay-Sevilla, H. García-Ortiz, M. Gross, S. Han, N. L. Heard-Costa, A. U. Jackson, M. E. Jørgensen, H. M. Kang, M. Kelsey, B. J. Kim, H. A. Koistinen, J. Kuusisto, J. B. Leader, A. Linneberg, C. T. Liu, J. Liu, V. Lyssenko, A. K. Manning, A. Marcketta, J. M. Malacara-Hernandez, A. Martínez-Hernández, K. Matsuo, E. Mayer-Davis, E. Mendoza-Caamal, K. L. Mohlke, A. C. Morrison, A. Ndungu, M. C. Y. Ng, C. O'Dushlaine, A. J. Payne, C. Pihoker, W. S. Post, M. Preuss, B. M. Psaty, R. S. Vasan, N. W. Rayner, A. P. Reiner, C. Revilla-Monsalve, N. R. Robertson, N. Santoro, C. Schurmann, W. Y. So, X. Soberón, H. M. Stringham, T. M. Strom, C. H. T. Tam, F. Thameem, B. Tomlinson, J. M. Torres, R. P. Tracy, R. M. van Dam, M. Vujkovic, S. Wang, R. P. Welch, D. R. Witte, T. Y. Wong, G. Atzmon, N. Barzilai, J. Blangero, L. L. Bonnycastle, D. W. Bowden, J. C. Chambers, E. Chan, C. Y. Cheng, Y. S. Cho, F. S. Collins, P. S. de Vries, R. Duggirala, B. Glaser, C. Gonzalez, M. E. Gonzalez, L. Groop, J. S. Kooner, S. H. Kwak, M. Laakso, D. M. Lehman, P. Nilsson, T. D. Spector, E. S. Tai, T. Tuomi, J. Tuomilehto, J. G. Wilson, C. A. Aguilar-Salinas, E. Bottinger, B. Burke, D. J. Carey, J. C. N. Chan, J. Dupuis, P. Frossard, S. R. Heckbert, M. Y. Hwang, Y. J. Kim, H. L. Kirchner, J. Y. Lee, J. Lee, R. J. F. Loos, R. C. W. Ma, A. D. Morris, C. J. O'Donnell, C. N. A. Palmer, J. Pankow, K. S. Park, A. Rasheed, D. Saleheen, X. Sim, K. S. Small, Y. Y. Teo, C. Haiman, C. L. Hanis, B. E. Henderson, L. Orozco, T. Tusié-Luna, F. E. Dewey, A. Baras, C. Gieger, T. Meitinger, K. Strauch, L. Lange, N. Grarup, T. Hansen, O. Pedersen, P. Zeitler, D. Dabelea, G. Abecasis, G. I. Bell, N. J. Cox, M. Seielstad, R. Sladek, J. B. Meigs, S. S. Rich, J. I. Rotter, D. Altshuler, N. P. Burtt, L. J. Scott, A. P. Morris, J. C. Florez, M. I. McCarthy, M. Boehnke, Exome sequencing of 20,791 cases of type 2 diabetes and 24,440 controls. *Nature* **570**, 71–76 (2019).
71. C. De Wit, F. Roos, S. S. Bolz, U. Pohl, Lack of vascular connexin 40 is associated with hypertension and irregular arteriolar vasomotion. *Physiol. Genomics* **13**, 169–177 (2003).
72. M. Firouzi, B. Kok, W. Spiering, A. Busjahn, C. R. Bezzina, J. M. Ruijter, B. P. C. Koeleman, M. Schipper, W. A. Groenewegen, H. J. Jongsma, P. W. De Leeuw, Polymorphisms in human connexin40 gene promoter are associated with increased risk of hypertension in men. *J. Hypertens.* **24**, 325–330 (2006).
73. M. A. Gebska, B. K. Stevenson, A. R. Hemnes, T. J. Bivalacqua, A. Haile, G. G. Hesketh, C. I. Murray, A. L. Zaiman, M. K. Halushka, N. Krongkaew, T. D. Strong, C. A. Cooke, H. El-Haddad, R. M. Tuder, D. E. Berkowitz, H. C. Champion, Phosphodiesterase-5A (PDE5A) is localized to the endothelial caveolae and modulates NOS3 activity. *Cardiovasc. Res.* **90**, 353–363 (2011).
74. H. C. Thiesson, B. L. Jensen, B. Jespersen, O. B. Schaffalitzky De Muckadell, C. Bistrup, S. Walter, P. D. Ottosen, A. Veje, O. Skøtt, Inhibition of cGMP-specific phosphodiesterase type 5 reduces sodium excretion and arterial blood pressure in patients with NaCl retention and ascites. *Am. J. Physiol. Renal. Physiol.* **288**, 1044–1052 (2005).
75. E. Sohara, Y. Luo, J. Zhang, D. K. Manning, D. R. Beier, J. Zhou, Nek8 regulates the expression and localization of polycystin-1 and polycystin-2. *J. Am. Soc. Nephrol.* **19**, 469–476 (2008).
76. G. Büyükdereli, I. B. Guney, M. Kibar, C. Kinaci, Thyroid hemiagenesis: A report of three cases and review of the literature. *Ann. Nucl. Med.* **19**, 147–150 (2005).
77. S. W. M. John, A. T. Veress, U. Honrath, C. K. Chong, L. Peng, O. Smithies, H. Sonnenberg, Blood pressure and fluid-electrolyte balance in mice with reduced or absent ANP. *Am. J. Physiol.* **271**, R109–R114 (1996).
78. L. Yao, J. He, B. Li, M. Yan, H. Wang, L. Tan, M. Liu, X. Lv, H. Lv, X. Zhang, C. Chen, D. Wang, Y. Yu, Y. Huang, Y. Zhu, D. Ai, Regulation of YAP by mammalian target of rapamycin complex 1 in endothelial cells controls blood pressure through COX-2/mPGES-1/PGE2 cascade. *Hypertension* **74**, 936–946 (2019).

79. A. Astrand, M. Bohlooly-Y, S. Larsdotter, M. Mahlapuu, H. Andersén, J. Tornell, C. Ohlsson, M. Snaith, D. G. A. Morgan, Mice lacking melanin-concentrating hormone receptor 1 demonstrate increased heart rate associated with altered autonomic activity. *Am. J. Physiol. Regul. Integr. Comp. Physiol.* **287**, R749–R758 (2004).
80. R. B. Williams, G. D. Bishop, B. C. Haberstick, A. Smolen, B. H. Brummett, I. C. Siegler, M. A. Babyak, X. Zhang, E. S. Tai, J. J. M. Lee, M. Tan, Y. Y. Teo, S. Cai, E. Chan, C. T. Halpern, E. A. Whitsel, S. Bauldry, K. M. Harris, Population differences in associations of serotonin transporter promoter polymorphism (5HTTLPR) di- and triallelic genotypes with blood pressure and hypertension prevalence. *Am. Heart J.* **185**, 110–122 (2017).
81. W. L. Miller, Mechanisms in endocrinology: Rare defects in adrenal steroidogenesis. *Eur. J. Endocrinol.* **179**, R125–R141 (2018).
82. D. A. Braun, C. E. Sadowski, S. Kohl, S. Lovric, S. A. Astrinidis, W. L. Pabst, H. Y. Gee, S. Ashraf, J. A. Lawson, S. Shril, M. Airik, W. Tan, D. Schapiro, J. Rao, W. Il Choi, T. Hermle, M. J. Kemper, M. Pohl, F. Ozaltin, M. Konrad, R. Bogdanovic, R. Büscher, U. Helmchen, E. Serdaroglu, R. P. Lifton, W. Antonin, F. Hildebrandt, Mutations in nuclear pore genes NUP93, NUP205 and XPO5 cause steroid-resistant nephrotic syndrome. *Nat. Genet.* **48**, 457–465 (2016).
83. A. E. Linder, J. Diaz, W. Ni, T. Szasz, R. Burnett, S. W. Watts, Vascular reactivity, 5-HT uptake, and blood pressure in the serotonin transporter knockout rat. *Am. J. Physiol. Heart Circ. Physiol.* **294**, 1745–1752 (2008).
84. C. R. Lake, P. B. Davis, M. Ziegler, I. J. Kopin, Electrolytes and norepinephrine levels in blood of patients with cystic fibrosis. *Clin. Chim. Acta* **92**, 141–146 (1979).
85. J. Yang, V. Singh, B. Cha, T. E. Chen, R. Sarker, R. Murtazina, S. Jin, N. C. Zachos, G. H. Patterson, C. M. Tse, O. Kovbasnjuk, X. Li, M. Donowitz, NHERF2 protein mobility rate is determined by a unique C-terminal domain that is also necessary for its regulation of NHE3 protein in OK cells. *J. Biol. Chem.* **288**, 16960–16974 (2013).
86. J. D. Backman, A. H. Li, A. Marcketta, D. Sun, J. Mbatchou, M. D. Kessler, C. Benner, D. Liu, A. E. Locke, S. Balasubramanian, A. Yadav, N. Banerjee, C. E. Gillies, A. Damask, S. Liu, X. Bai, A. Hawes, E. Maxwell, L. Gurski, K. Watanabe, J. A. Kosmicki, V. Rajagopal, J. Mighty, M. Jones, L. Mitnaul, E. Stahl, G. Coppola, E. Jorgenson, L. Habegger, W. J. Salerno, A. R. Shuldiner, L. A. Lotta, J. D. Overton, M. N. Cantor, J. G. Reid, G. Yancopoulos, H. M. Kang, J. Marchini, A. Baras, G. R. Abecasis, M. A. R. Ferreira, Exome sequencing and analysis of 454,787 UK Biobank participants. *Nature* **599**, 628–634 (2021).
87. S. E. Simonds, J. T. Pryor, E. Ravussin, F. L. Greenway, R. Dileone, A. M. Allen, J. Bassi, J. K. Elmquist, J. M. Keogh, E. Henning, M. G. Myers, J. Licinio, R. D. Brown, P. J. Enriori, S. O'Rahilly, S. M. Sternson, K. L. Grove, D. C. Spanswick, I. S. Farooqi, M. A. Cowley, Leptin mediates the increase in blood pressure associated with obesity. *Cell* **159**, 1404–1416 (2014).
88. Q. Wu, J. Zhang, W. Koh, Q. Yu, X. Zhu, A. Amsterdam, G. E. Davis, M. A. Arnaout, J. W. Xiong, Talin1 is required for cardiac Z-disk stabilization and endothelial integrity in zebrafish. *FASEB J.* **29**, 4989–5005 (2015).
89. A. M. Manso, H. Okada, F. M. Sakamoto, E. Moreno, S. J. Monkley, R. Li, D. R. Critchley, R. S. Ross, Loss of mouse cardiomyocyte talin-1 and talin-2 leads to β-1 integrin reduction, costameric instability, and dilated cardiomyopathy. *Proc. Natl. Acad. Sci. U.S.A.* **114**, E6250–E6259 (2017).
90. X. C. Duan, S. Y. Liu, R. Guo, L. Xiao, H. M. Xue, Q. Guo, S. Jin, Y. M. Wu, Cystathionine-β-synthase gene transfer into rostral ventrolateral medulla exacerbates hypertension via nitric oxide in spontaneously hypertensive rats. *Am. J. Hypertens.* **28**, 1106–1113 (2015).
91. X. C. Duan, R. Guo, S. Y. Liu, L. Xiao, H. M. Xue, Q. Guo, S. Jin, Y. M. Wu, Gene transfer of cystathionine β-synthase into RVLM increases hydrogen sulfide-mediated suppression of sympathetic outflow via KATP channel in normotensive rats. *Am J. Physiol. Heart Circ. Physiol.* **308**, H603–H611 (2015).
92. J. Kuß, B. Stallmeyer, M. Goldstein, S. Rinné, C. Pees, S. Zumhagen, G. Seebohm, N. Decher, L. Pott, M. C. Kienitz, E. Schulze-Bahr, Familial sinus node disease caused by a gain of GIRK (G-protein activated inwardly rectifying K^+ channel) channel function. *Circ. Genom. Precis. Med.* **12**, e002238 (2019).
93. J. Bollerslev, E. Sjöstedt, L. Rejnmark, Cardiovascular consequences of parathyroid disorders in adults. *Ann. Endocrinol.* **82**, 151–157 (2021).
94. Z. Liu, S. Yu, N. R. Manley, Gcm2 is required for the differentiation and survival of parathyroid precursor cells in the parathyroid/thymus primordia. *Dev. Biol.* **305**, 333–346 (2007).
95. L. Marger, P. Mesirca, J. Alig, A. Torrente, S. Dubel, B. Engeland, S. Kanani, P. Fontanaud, J. Striessnig, H. S. Shin, D. Isbrandt, H. Ehmke, J. Nargeot, M. E. Mangoni, Functional roles of $Ca_v1.3$, $Ca_v3.1$ and HCN channels in automaticity of mouse atrioventricular cells. *Channels* **5**, 251–261 (2011).
96. P. Mesirca, J. Alig, A. G. Torrente, J. C. Müller, L. Marger, A. Rollin, C. Marquilly, A. Vincent, S. Dubel, I. Bidaud, A. Fernandez, A. Seniuk, B. Engeland, J. Singh, L. Miquerol, H. Ehmke, T. Eschenhagen, J. Nargeot, K. Wickman, D. Isbrandt, M. E. Mangoni, Cardiac arrhythmia induced by genetic silencing of "funny" (*f*) channels is rescued by *GIRK4* inactivation. *Nat. Commun.* **5**, 4664 (2014).
97. R. Shaheen, E. Faqeih, M. J. Alshammari, A. Swaid, L. Al-Gazali, E. Mardawi, S. Ansari, S. Sogaty, M. Z. Seidahmed, M. I. Almotairi, C. Farra, W. Kurdi, S. Al-Rasheed, F. S. Alkuraya, Genomic analysis of Meckel-Gruber syndrome in Arabs reveals marked genetic heterogeneity and novel candidate genes. *Eur. J. Hum. Genet.* **21**, 762–768 (2013).
98. D. Shigemizu, T. Aiba, H. Nakagawa, K. Ozaki, F. Miya, W. Satake, T. Toda, Y. Miyamoto, A. Fujimoto, Y. Suzuki, M. Kubo, T. Tsunoda, W. Shimizu, T. Tanaka, Exome analyses of long QT syndrome reveal candidate pathogenic mutations in calmodulin-interacting genes. *PLOS ONE* **10**, e0130329 (2015).
99. D. Labonté, E. Thies, M. Kneussel, The kinesin KIF21B participates in the cell surface delivery of γ2 subunit-containing GABAA receptors. *Eur. J. Cell Biol.* **93**, 338–346 (2014).
100. S. Bazrafshan, H. Kushlaf, M. Kakroo, J. Quinlan, R. C. Becker, S. Sadayappan, Genetic modifiers of hereditary neuromuscular disorders and cardiomyopathy. *Cell* **10**, 1–19 (2021).
101. T. R. Grossman, A. Gamliel, R. J. Wessells, O. Taghli-Lamallem, K. Jepsen, K. Ocorr, J. R. Korenberg, K. L. Peterson, M. G. Rosenfeld, R. Bodmer, E. Bier, Over-expression of DSCAM and COL6A2 cooperatively generates congenital heart defects. *PLOS Genet.* **7**, e1002344 (2011).
102. P. Stijnen, B. Ramos-Molina, S. O'Rahilly, J. W. M. Creemers, PCSK1 mutations and human endocrinopathies: From obesity to gastrointestinal disorders. *Endocr. Rev.* **37**, 347–371 (2016).
103. Z. C. Wang, W. H. Ji, C. W. Ruan, X. Y. Liu, X. B. Qiu, F. Yuan, R. G. Li, Y. J. Xu, X. Liu, R. T. Huang, S. Xue, Y. Q. Yang, Prevalence and spectrum of TBX5 mutation in patients with lone atrial fibrillation. *Int. J. Med. Sci.* **13**, 60–67 (2016).
104. D. Tamuli, M. Kaur, A. Boligarla, A. K. Jaryal, A. K. Srivastava, K. K. Deepak, Depressed baroreflex sensitivity from spontaneous oscillations of heart rate and blood pressure in SCA1 and SCA2. *Acta Neurol. Scand.* **140**, 350–358 (2019).
105. C. Roselli, M. D. Chaffin, L. C. Weng, S. Aeschbacher, G. Ahlberg, C. M. Albert, P. Almgren, A. Alonso, C. D. Anderson, K. G. Aragam, D. E. Arking, J. Barnard, T. M. Bartz, E. J. Benjamin, N. A. Bihlmeyer, J. C. Bis, H. L. Bloom, E. Boerwinkle, E. B. Bottinger, J. A. Brody, H. Calkins, A. Campbell, T. P. Cappola, J. Carlquist, D. I. Chasman, L. Y. Chen, Y. D. I. Chen, E. K. Choi, S. H. Choi, I. E. Christophersen, M. K. Chung, J. W. Cole, D. Conen, J. Cook, H. J. Crijns, M. J. Cutler, S. M. Damrauer, B. R. Daniels, D. Darbar, G. Delgado, J. C. Denny, M. Dichgans, M. Dörr, E. A. Dudink, S. C. Dudley, N. Esa, T. Esko, M. Eskola, D. Fatkin, S. B. Felix, I. Ford, O. H. Franco, B. Geelhoed, R. P. Grewal, V. Gudnason, X. Guo, N. Gupta, S. Gustafsson, R. Gutmann, A. Hamsten, T. B. Harris, C. Hayward, S. R. Heckbert, J. Hernesniemi, L. J. Hocking, A. Hofman, A. R. V. R. Horimoto, J. Huang, P. L. Huang, J. Huffman, E. Ingelsson, E. G. Ipek, K. Ito, J. Jimenez-Conde, R. Johnson, J. W. Jukema, S. Kääb, M. Kähönen, Y. Kamatani, J. P. Kane, A. Kastrati, S. Kathiresan, P. Katschnig-Winter, M. Kavousi, T. Kessler, B. L. Kietselaer, P. Kirchhof, M. E. Kleber, S. Knight, J. E. Krieger, M. Kubo, L. J. Launer, J. Laurikka, T. Lehtimäki, K. Leineweber, R. N. Lemaitre, M. Li, H. E. Lim, H. J. Lin, H. Lin, L. Lind, C. M. Lindgren, M. L. Lokki, B. London, R. J. F. Loos, S. K. Low, Y. Lu, L. P. Lyytikäinen, P. W. Macfarlane, P. K. Magnusson, A. Mahajan, R. Malik, A. J. Mansur, G. M. Marcus, L. Margolin, K. B. Margulies, W. März, D. D. McManus, O. Melander, S. Mohanty, J. A. Montgomery, M. P. Morley, A. P. Morris, M. Müller-Nurasyid, A. Natale, S. Nazarian, B. Neumann, C. Newton-Cheh, M. N. Niemeijer, K. Nikus, P. Nilsson, R. Noordam, H. Oellers, M. S. Olesen, M. Orho-Melander, S. Padmanabhan, H. N. Pak, G. Paré, N. L. Pedersen, J. Pera, A. Pereira, D. Porteous, B. M. Psaty, S. L. Pulit, C. R. Pullinger, D. J. Rader, L. Refsgaard, M. Ribasés, P. M. Ridker, M. Rienstra, L. Risch, D. M. Roden, J. Rosand, M. A. Rosenberg, N. Rost, J. I. Rotter, S. Saba, R. K. Sandhu, R. B. Schnabel, K. Schramm, H. Schunkert, C. Schurman, S. A. Scott, I. Seppälä, C. Shaffer, S. Shah, A. A. Shalaby, J. Shim, M. B. Shoemaker, J. E. Siland, J. Sinisalo, M. F. Sinner, A. Slowik, A. V. Smith, B. H. Smith, J. G. Smith, J. D. Smith, N. L. Smith, E. Z. Soliman, N. Sotoodehnia, B. H. Stricker, A. Sun, H. Sun, J. H. Svendsen, T. Tanaka, K. Tanriverdi, K. D. Taylor, M. Teder-Laving, A. Teumer, S. Thériault, S. Trompet, N. R. Tucker, A. Tveit, A. G. Uitterlinden, P. van der Harst, I. C. van Gelder, D. R. van Wagoner, N. Verweij, E. Vlachopoulou, U. Völker, B. Wang, P. E. Weeke, B. Weijs, R. Weiss, S. Weiss, Q. S. Wells, K. L. Wiggins, J. A. Wong, D. Woo, B. B. Worrall, P. S. Yang, J. Yao, Z. T. Yoneda, T. Zeller, L. Zeng, S. A. Lubitz, K. L. Lunetta, P. T. Ellinor, Multi-ethnic genome-wide association study for atrial fibrillation. *Nat. Genet.* **50**, 1225–1233 (2018).
106. S. Fenske, S. C. Krause, S. I. H. Hassan, E. Becirovic, F. Auer, R. Bernard, C. Kupatt, P. Lange, T. Ziegler, C. T. Wotjak, H. Zhang, V. Hammelmann, C. Paparizos, M. Biel, C. A. Wahl-Schott, Sick sinus syndrome in HCN1-deficient mice. *Circulation* **128**, 2585–2594 (2013).
107. C. Y. L. Huh, M. Danik, F. Manseau, L. E. Trudeau, S. Williams, Chronic exposure to nerve growth factor increases acetylcholine and glutamate release from cholinergic neurons of the rat medial septum and diagonal band of broca via mechanisms mediated by p75NTR. *J. Neurosci.* **28**, 1404–1409 (2008).
108. C. C. Chang, W. H. Fang, H. A. Chang, S. Y. Huang, Functional *Ser205Leu* polymorphism of the nerve growth factor receptor (*NGFR*) gene is associated with vagal autonomic dysregulation in humans. *Sci. Rep.* **5**, 13136 (2015).
109. Y. Wang, J. Yin, C. Wang, H. Hu, X. Li, M. Xue, J. Liu, W. Cheng, Y. Wang, Y. Li, Y. Shi, J. Tan, X. Li, F. Liu, Q. Liu, S. Yan, Microglial Mincle receptor in the PVN contributes to sympathetic hyperactivity in acute myocardial infarction rat. *J. Cell. Mol. Med.* **23**, 112–125 (2019).
110. Y. H. Wang, L. Fu, B. Wang, S. F. Li, Z. Sun, Y. Luan, Genetic variants of interleukin-18 are associated with reduced risk of atrial fibrillation in a population from Northeast China. *Gene* **626**, 269–274 (2017).

111. T. Berg, M-currents (Kv7.2-7.3/KCNQ2-KCNQ3) are responsible for dysfunctional autonomic control in hypertensive rats. *Front. Physiol.* **7**, 584 (2016).
112. T. Unger, H. Becker, R. Dietz, D. Ganten, R. E. Lang, R. Rettig, A. Schomig, N. A. Schwab, Antihypertensive effect of the GABA receptor agonist muscimol in spontaneously hypertensive rats. Role of the sympathoadrenal axis. *Circ. Res.* **54**, 30–37 (1984).
113. H. I. Atasoy, E. Tug, T. Yavuz, N. Cine, Unique variant of Adams-Oliver syndrome with dilated cardiomyopathy and heart block. *Pediatr. Int.* **55**, 508–512 (2013).
114. K. M. Jones, A. Silfvast-Kaiser, D. R. Leake, L. Z. Diaz, M. L. Levy, Adams-Oliver syndrome type 2 in association with compound heterozygous DOCK6 mutations. *Pediatr. Dermatol.* **34**, e249–e253 (2017).
115. M. J. Bround, P. Asghari, R. B. Wambolt, L. Bohunek, C. Smits, M. Philit, T. J. Kieffer, E. G. Lakatta, K. R. Boheler, E. D. W. Moore, M. F. Allard, J. D. Johnson, Cardiac ryanodine receptors control heart rate and rhythmicity in adult mice. *Cardiovasc. Res.* **96**, 372–380 (2012).
116. S. Herrmann, P. Lipp, K. Wiesen, J. Stieber, H. Nguyen, E. Kaiser, A. Ludwig, The cardiac sodium-calcium exchanger NCX1 is a key player in the initiation and maintenance of a stable heart rhythm. *Cardiovasc. Res.* **99**, 780–788 (2013).
117. Z. Gao, T. P. Rasmussen, Y. Li, W. Kutschke, O. M. Koval, Y. Wu, Y. Wu, D. D. Hall, M. L. A. Joiner, X. Q. Wu, P. D. Swaminathan, A. Purohit, K. Zimmerman, R. M. Weiss, K. D. Philipson, L. S. Song, T. J. Hund, M. E. Anderson, Genetic inhibition of Na^+-$Ca2^+$ exchanger current disables fight or flight sinoatrial node activity without affecting resting heart rate. *Circ. Res.* **112**, 309–317 (2013).

Acknowledgments: We thank F. T. Sato and A. L. Americo for discussions. **Funding:** This work was supported by Fundação de Amparo à Pesquisa do Estado de São Paulo (FAPESP) grant nos. INCT–2014/50889-7 (to J.E.K.), 2013/17368-0 (to J.E.K.), 2015/50216-5 (to J.E.K.), BEPE–2017/1448-4 (to R.P.), and BCO–2017/05352-3 (to R.P.); Conselho Nacional de Desenvolvimento Científico e Tecnológico (CNPq) grant nos. INCT–465586/2014-7 (to J.E.K.), 309179/2013-0 (to J.E.K.), and 442643/2020-9 (to J.E.K.); and Coordenação de Aperfeiçoamento de Pessoal de Nível Superior (CAPES) grants 88882.328135/2019-01 (to S.K.T.) and PGCI–99999.000530/2016-06 (to S.K.T.). **Author contributions:** Conceptualization: S.K.T., B.B., and J.E.K. Methodology: S.K.T., R.P., L.F.G.Z., J.W., D.X., S.H., J.R., X.Z., M.C., M.T., X.L., and S.L. Investigation: S.K.T. Visualization: S.K.T. Supervision: S.K.T., B.B., and J.E.K. Writing—original draft: S.K.T. Writing—review and editing: S.K.T., B.B., and J.E.K. **Competing interests:** The authors declare that they have no competing interests. **Data and materials availability:** All data needed to evaluate the conclusions in the paper are present in the paper and/or the Supplementary Materials. Results and G1 mouse models are available upon request through the Mutagenetix website at https://mutagenetix.utsouthwestern.edu/home.cfm and through the Mutant Mouse Resource and Research Center (MMRRC), respectively. The *Zfp106*, *Kl*, *Nae1*, and *Notch3* KO and engineered mice were provided by B.B. under a material transfer agreement. Requests for the KO and engineered mice should be submitted to B.B.

Submitted 27 July 2023
Accepted 29 January 2024
Published 1 March 2024
10.1126/sciadv.adj9797